1 **Variations in the chemical composition of the submicron aerosol and in the**

2 **sources of the organic fraction at a regional background site of the Po Valley**

3 **(Italy)**

4

5 M. Bressi[1], F. Cavalli[1], C. A. Belis[1], J. -P. Putaud[1], R. Fröhlich[2], S. Martins dos Santos[1], E. Petralia[3], A. S.

6 H. Prévôt[2], M. Berico[3], A. Malaguti[3] and F. Canonaco[2]

7

8 [1]European Commission, Joint Research Centre, Institute for Environment and Sustainability, Air and

9 Climate Unit, Via Enrico Fermi 2749, Ispra (VA) 21027, Italy.

10 [2]Paul Scherrer Institute, Laboratory of Atmospheric Chemistry, Villigen 5232, Switzerland.

11 [3]Italian National Agency for New Technologies, Energy and Sustainable Economic Development (ENEA),

12 Via Martiri di Monte Sole 4, Bologna 40129, Italy.

13

14 Correspondence to:

15 michael.bressi@jrc.ec.europa.eu, claudio.belis@jrc.ec.europa.eu, fabrizia.cavalli@jrc.ec.europa.eu

16

17 **Abstract**

18 Fine particulate matter (PM) levels and resulting impacts on human health are in the Po Valley (Italy)

19 among the highest in Europe. To build effective PM abatement strategies, it is necessary to characterize

20 fine PM chemical composition, sources and atmospheric processes on long time scales (>months), with

21 short time resolution (<day), and with particular emphasis on the predominant organic fraction.

22 Although previous studies have been conducted in this region, none of them addressed all these aspects

23 together. For the first time in the Po Valley, we investigate the chemical composition of non-refractory

24 submicron PM (NR-PM$_1$) with a time-resolution of 30 minutes at the regional background site of Ispra

25 during one full year, using an Aerosol Chemical Speciation Monitor (ACSM) under the most up-to-date

26 and stringent quality assurance protocol. The identification of the main components of the organic

27 fraction is made using the Multilinear-Engine 2 algorithm implemented within the latest version of the

28 SoFi toolkit. In addition, with a view of a potential implementation of ACSM measurements in European

29 air quality networks as a replacement of traditional filter-based techniques, parallel multiple off-line

30 analyses were carried out to assess the performance of the ACSM in the determination of PM chemical

31 species regulated by Air Quality Directives. The annual NR-PM$_1$ level monitored at the study site (14.2

Atmospheric
Chemistry
and Physics
Discussions

Open Access

32   µg/m^3) is among the highest in Europe, and is even comparable to levels reported in urban areas like

33   New York City (USA, 14.2 µg/m^3) and Tokyo (Japan, 12-15 µg/m^3). On the annual basis, submicron

34   particles are primarily composed of organic aerosol (OA, 58% of NR-PM$_1$). This fraction was apportioned

35   into oxygenated OA (OOA, 66%), hydrocarbon-like OA (HOA, 11% of OA), and biomass burning OA

36   (BBOA, 23%). Among the primary sources of OA, biomass burning (23%) is thus bigger than fossil fuel

37   combustion (11%). Significant contributions of aged secondary organic aerosol (OOA) are observed

38   throughout the year. The unexpectedly high degree of oxygenation estimated during wintertime is

39   probably due to the contribution of secondary BBOA and the enhancement of aqueous phase

40   production of OOA during cold months. BBOA and nitrate are the only components of which

41   contributions increase with the NR-PM$_1$ levels. Therefore, biomass burning and NO$_x$ emission reductions

42   would be particularly efficient in limiting submicron aerosol pollution events. Abatement strategies

43   conducted during cold seasons appear to be more efficient than annual-based policies. In a broader

44   context, further studies using high-time resolution analytical techniques on a long-term basis for the

45   characterization of fine aerosol should help better shape our future air quality policies, which constantly

46   need refinement.

47

48   1. Introduction

49   The Po Valley region - located in northern Italy - is amongst the most polluted areas in Europe (van

50   Donkelaar et al., 2010; EEA, 2013). Annual PM$_{2.5}$ (particulate matter with an aerodynamic diameter

51   below 2.5 µm) mean concentrations can significantly exceed the European PM$_{2.5}$ annual limit value (25

52   µg/m^3 in 2015, European Directive 2008/50/EC) and the recommendations of the World Health

53   Organization (PM$_{2.5}$ annual average of 10 µg/m^3; WHO, 2006) at urban (e.g. Bologna, 35.8 µg/m^3) and

54   regional background sites (e.g. Ispra, 32.2 µg/m^3; Putaud et al., 2010). Consequently, PM$_{2.5}$ impacts on

55   human health are among the most severe in Europe (EC, 2005), while impacts on the local radiative

56   forcing are substantial (Clerici and Mélin, 2008; Ferrero et al., 2014; Putaud et al., 2014b). Effective PM

57   abatement strategies are thus needed in the Po Valley and require an in-depth knowledge of the

58   chemical composition of fine PM, to quantify its sources and the atmospheric processes leading to its

59   secondary formation.

60   In this region, high levels of fine aerosol are mostly due to the conjunction of i) high pollutant

61   emissions related to industrial, transport, biomass burning and agricultural activities - the Po river basin

62   hosting 37% of the Italian industries, 55% of the livestock and contributing 35% of the Italian agricultural

63   production (WMO et al., 2012) - and ii) the specific geography and topography of this area - a flat basin

Atmospheric
Chemistry
and Physics
Discussions

Open Access

EGU

64   surrounded by the Alps and Apennine Mountains dominated by weak winds that favour the

65   accumulation of pollutants (Decesari et al., 2014; Kukkonen et al., 2005; Pernigotti et al., 2012). As a

66   consequence, PM levels are not only high in urban areas but also at regional and rural background sites,

67   which are key locations for investigating air pollution due to their distance from local sources and local

68   phenomena. Measurements of fine PM mass and chemical composition at rural background sites are in

69   addition specifically required in the current European Directive on air quality (2008/50/EC).

70   Previous studies have investigated the properties of fine aerosols at regional and rural

71   background sites of the Po valley region, including their chemical characteristics (e.g. Carbone et al.,

72   2014; Putaud et al., 2002, 2010; Saarikoski et al., 2012), and their main sources (Belis et al., 2013;

73   Gilardoni et al., 2011; Larsen et al., 2012; Perrone et al., 2012). Fine aerosols are primarily made of

74   organics (30-80% of fine PM mass, depending on the site and season studied), followed by ammonium

75   nitrate and ammonium sulfate. Their main sources are fossil fuel, biomass burning and biogenic

76   emissions to name a few. In studies dealing with long time-series (entire season or year), the chemical

77   composition of fine aerosol is generally measured with a relatively low time resolution (typically 24

78   hours), thus preventing from studying its diurnal variation and short-lived chemical-physical processes.

79   When documented with higher time-resolutions (1 hour or less), aerosol chemistry is usually

80   determined for intensive campaigns of a few weeks only, hence not suitable to depict the seasonal or

81   yearly air quality situation. In addition, the complexity of the fine organic fraction (e.g. Jimenez et al.,

82   2009) requires state-of-the-art analytical and source apportionment (SA) techniques to identify organic

83   aerosol chemical properties and sources.

84   The recently developed Aerosol Chemical Speciation Monitor (ACSM, Aerodyne Research Inc.,

85   Ng et al., 2011a) is suitable to fill these gaps by providing the chemical composition of non-refractory

86   submicron aerosols (NR-PM$_1$) with a time resolution of 30 min, while operating on long time scales. Even

87   though promising results have been recently reported (e.g. Budisulistiorini et al., 2014; Canonaco et al.,

88   2013, 2015; Minguillón et al., 2015; Ng et al., 2011a; Petit et al., 2015; Ripoll et al., 2015; Sun et al.,

89   2012), this technique remains recent and requires additional field deployment to test its consistency

90   with independent methods for the monitoring of fine PM chemistry (e.g. filter measurements). In

91   addition, information on the accuracy of this technique is of paramount importance given the growing

92   number of ACSMs in Europe and the necessity to build a network of quality assured and harmonized

93   instruments for comparability of results – at present about 20 ACSMs are in operation in Europe

94   (http://www.psi.ch/acsm-stations/overview-full-period) within the frame of the EU ACTRIS network

95   (Aerosols, Clouds, and Traces gases Research InfraStructure, http://www.actris.eu/). Moreover, by using

Atmospheric
Chemistry
and Physics
Discussions

96   receptor models, the apportionment of organic aerosol (OA) into its major components - hydrocarbon-

97   like (HOA), biomass burning (BBOA) and oxygenated OA (OOA) - can be performed (Lanz et al., 2007;

98   Zhang et al., 2011 and references therein).

99   In this study, we used an ACSM during one year with a 30 min time-resolution at a regional

100   background site of the Po Valley and performed subsequent SA analyses with the aim of: i) describing

101   the high time resolved chemical composition of NR-PM$_1$ on a long time-scale, to better understand the

102   physicochemical processes driving its temporal variations, ii) apportioning the organic fraction into its

103   main sources, iii) identifying PM abatement strategies to efficiently reduce NR-PM$_1$ pollution events at

104   regional background areas of the Po valley, and iv) assessing the atmospheric consistency of ACSM

105   measurements when compared to independent analytical methods, to evaluate its possible

106   implementation in future European Air Quality networks.

107

108   2.   Material and methods

109   2.1. Sampling site

110   Measurements were conducted at the European Commission – Joint Research Centre (EC-JRC) Ispra site

111   (45°48'N, 8°38'E, 217 m a.s.l.), which is part of the European Monitoring and Evaluation Programme

112   (EMEP) measurement network (http://www.nilu.no/projects/ccc/ sitedescriptions/it/index.html) and

113   the   Global   Atmosphere   Watch   (GAW)   regional   stations

114   (http://www.wmo.int/pages/prog/arep/gaw/measurements.html). It is located on the northwest edge

115   of the Po Valley region, 60 km northwest of the Milan urban area. It can be regarded as a "regional/rural

116   background" site following the criteria recommended by the European Environment Agency (Larssen et

117   al., 1999). For simplicity, the term "regional background site" will be used in the following although

118   comparisons with rural background sites from other studies will also be reported. Further information

119   on the study site can be found in Putaud et al. (2014b).

120

121   2.2. Aerosol Chemical Speciation Monitor (ACSM)

122   The recently developed ACSM (Aerodyne Research Inc., ARI) was used to measure the non-refractory

123   (NR) chemical composition (organics, nitrate, sulfate, ammonium, chloride) of submicron particles (PM$_1$)

124   with a 30 minutes time resolution. The operating principle of the ACSM is similar to the widespread

125   Aerodyne aerosol mass spectrometer (Canagaratna et al., 2007; Jayne et al., 2000), with the difference

126   that the former does not inform on the size distribution of the chemical composition of NR-PM$_1$. A full

127   description of the ACSM can be found in Ng et al. (2011a). Briefly, an aerodynamic lens is used to focus

Atmospheric
Chemistry
and Physics
Discussions

Open Access

EGU

128   submicron particles (50% transmission range of 75-650 nm; Liu et al., 2007), which are then vaporized in

129   high vacuum, ionized by electron ionization (at 70eV) and detected by a quadrupole mass spectrometer

130   (Pfeiffer Vacuum Prisma Plus RGA). Two different quadrupole-ACSMs (Q-ACSMs) were used in this study

131   (from March 2013 to February 2014): Q-ACSM#1 from 01 March to 18 August 2013 and Q-ACSM#2 from

132   20 June 2013 to 28 February 2014. Note that Q-ACSM#2 was not running from 3 November to 18

133   December due to its participation in the first inter-ACSM comparison exercise (Crenn et al., 2015). The

134   reproducibility and consistency with independent measurements are discussed in Sect. 3.1. In the

135   following, orthogonal regressions are reported unless otherwise stated.

136   Both ACSMs were operated with the latest Data Acquisition (DAQ 1.4.3.8 to 1.4.4.5) and Data

137   Analysis (DAS 1.5.3.0 to 1.5.3.2) software (ARI, https://sites.google.com/site/ariacsm/mytemplate-sw)

138   available at the time of use, which are developed within Igor Pro 6.32A (Wavemetrics).

139   Recommendations given by Aerodyne (2010a, 2010b) and Ng et al. (2011a) were followed for the

140   operation, calibration and data analysis of the ACSMs. Ammonium nitrate calibrations were performed

141   seasonally and used for the determination of experimental nitrate response factors (RF) and ammonium

142   relative ionization efficiencies (RIE, see Sect. S1 for further details). Annual average and season-

143   dependent experimental RF and RIE values were alternatively applied to assess whether the ACSM is

144   stable over multi-seasonal periods (see Sect. 3.1 for results). RIEs for organics, nitrate and chloride (1.4,

145   1.1 and 1.3, respectively) were taken from the literature (Canagaratna et al., 2007; Takegawa et al.,

146   2005). RIE for sulfate was experimentally determined based on ammonium sulfate calibrations for

147   ACSM#2, and was taken from the literature for ACSM#1 (see Sect. S1). Collection efficiencies (CE) set as

148   i) a fixed 0.5 value (e.g. Budisulistiorini et al., 2013) or ii) following the composition-dependent CE

149   algorithm introduced by Middlebrook et al. (2012) were compared in order to determine the most

150   appropriate CEs (see Sect. 3.1 for results).

151

152   2.3. Additional analytical techniques

153   Additional measurements routinely performed at the JRC-Ispra site are used in this study (see Putaud et

154   al., 2014a for a full description). $PM_{2.5}$ are sampled on quartz fibre filters (Pall, 2500 QAT-UP) with a

155   Partisol PLUS 2025 sampler equipped with a carbon honeycomb denuder operating at 16.7 L/min from

156   01 March 2013 to 28 February 2014 with daily filter changes at 08:00 UTC. Major ions (NH_4^+, K^+, NO_3^-,

157   SO_4^{2-}, etc.) are analysed by ion chromatography (Dionex DX 120 with electrochemical eluent

158   suppression) after extraction in Milli-Q water (Millipore). Organic and elemental carbon (OC and EC,

159   respectively) are quantified by a thermal-optical method (Sunset Dual-optical Lab Thermal-Optical

Atmospheric
Chemistry
and Physics
Discussions

160   Carbon Aerosol Analyzer) using the EUSAAR-2 protocol (Cavalli et al., 2010). Equivalent Black Carbon

161   (BC) is measured by a Multi Angle Absorption Photometer (MAAP, Thermo Scientific, model 5012)

162   applying an absorption cross section of 6.6 m^2/g of equivalent black carbon at the operation wavelength

163   of 670 nm. Particle volume concentrations are determined with a home-made Differential Mobility

164   Particle Sizer (DMPS) combining a Vienna-type Differential Mobility Analyser (DMA) and a Condensation

165   Particle Counter (CPC, TSI 3010), following the European Supersites for Atmospheric Aerosol Research

166   (EUSAAR) specifications for DMPS systems (Wiedensohler et al., 2012). Meteorological variables

167   (temperature, pressure, relative humidity, precipitation, wind speed and direction) are determined from

168   a weather transmitter WXT510 (Vaisala, Finland). Solar radiation is measured by a CM11 pyranometer

169   (Kipp and Zonen, The Netherlands).

170

171   2.4. Apportionment of the organic fraction

172   The organic fraction was apportioned using the Positive Matrix Factorization approach (PMF, Lanz et al.,

173   2007; Paatero and Tapper, 1994; Ulbrich et al., 2009; Zhang et al., 2011) by applying the Multilinear

174   Engine 2 algorithm (ME-2, Paatero, 2000) implemented in the SoFi tool (v4.8, Canonaco et al., 2013;

175   Crippa et al., 2014). Details on the theory and application of PMF and ME-2 can be found in the

176   aforementioned studies. Briefly PMF aims at factorizing an initial X matrix (representing the temporal

177   variation of *m/z* signals here) into two F and G matrices (representing factor profiles and contributions,

178   respectively) putting a constraint of non-negativity on F and G matrices. Contrary to classical program

179   used to resolve PMF, ME-2 allows any element of the F and G matrices to be constrained with a certain

180   degree of freedom. This ME-2 approach has been typically used to constrain full factor profiles (e.g.

181   Amato et al., 2009; Crippa et al., 2014), specific elemental ratios (e.g. Sturtz et al., 2014) or specific

182   species contribution (e.g. Crawford et al., 2005) in a given factor profile.

183   In our study, ME-2 is applied with and without constraining factor profiles (FPs), using the so-

184   called *a*-value approach (Canonaco et al., 2013) in the former case, which can be described as follows:

185    $(f_{k,j})_{solution} = (f_{k,j})_{reference} \pm a \cdot (f_{k,j})_{reference}$ (1)

186   where k and j are the indexes for the factors and the species, respectively, $f_{k,j}$ is the element (k, j) of the

187   F matrix, the index "solution" stands for the PMF user solution, "reference" for the reference profile and

188   "*a*" is a scalar defined between 0 and 1 (e.g. applying an *a*-value of 0.10 lets ±10% variability to our FP

189   solution with respect to the reference FP). Following Crippa et al. (2014), we perform a sequence of runs

190   with i) unconstrained PMF, ii) fixed HOA, iii) fixed HOA and BBOA, iv) fixed HOA, BBOA and cooking OA

191   (COA) factors before selecting the most appropriate solution. Uncertainties are calculated using the DAS

Atmospheric
Chemistry
and Physics
Discussions

192   1.5.3.0 version following the methodologies of Allan et al., 2003a and Ulbrich et al. (2009). *m/z* 12 and

193   13 are removed for SA analysis since negative signals are observed most of the time. Reference factor

194   profiles (RFPs) are taken from ambient deconvolved spectra from the Aerosol Mass Spectrometry (AMS)

195   spectral database (Ulbrich et al., 2015). HOA and BBOA profiles are taken from Ng et al. (2011c) (average

196   of profiles from multiple studies) and COA from Crippa et al. (2013). Different *a*-values are tested (see

197   Sect. 3.2) applying i) relative standard deviations of averaged RFPs defined for every *m/z* (i.e. assuming

198   that the chosen averaged RFPs are representative of our data set), ii) recommendations of Crippa et al.

199   (2014) based on the SA of 25 European AMS data sets and iii) comparison with independent

200   measurements (e.g. NOx, CO, BC, etc.). Solutions from 2 to 8 factors are investigated in order to choose

201   the appropriate number of factors (see Sect. S2 and 3.2).

202

203   3. Results

204   3.1. Consistency of ACSM measurements

205   Ammonium nitrate calibrations performed on each ACSM are shown in

206   Figure S1. RF_{NO3} and RIE_{NH4} do not present significant seasonal variability - e.g. for ACSM#2 RF_{NO3}=4.7E-

207   11±0.2E-11 $A.\mu g^{-1}.m^3$ - , suggesting constant calibration factors may be used throughout the campaign.

208   On the other hand, calibration factors exhibit substantial discrepancies between both ACSMs (e.g. RF_{NO3}

209   of 2.5E-11 and 4.7E-11 $A.\mu g^{-1}.m^3$ for ACSM#1 and #2, respectively), suggesting that instrument-specific

210   factors are necessary. Applying constant and composition-dependent CEs does not lead to noticeable

211   differences (e.g. for NR-PM$_1$: r^2=0.97, slope=1.00±0.00, y-intercept=0.10±0.03 $\mu g/m^3$, n=14842) due to i)

212   low sampling line RH (e.g. typically below 30% for ACSM#2), and ii) few high-nitrate-content events (only

213   5% of data exhibits ammonium nitrate mass fractions>40%, defined as high by Middlebrook et al., 2012).

214   The Middlebrook et al. (2012) algorithm is however preferred since slightly acidic aerosols are observed

215   at the study site (on average sulfate plus nitrate against ammonium in $\mu eq/m^3$: r^2=0.96,

216   slope=1.21±0.00, intercept=0.01±0.00 $\mu eq/m^3$, n=14842).

217   A comparison performed between the two ACSMs used in this study during a 2-month summer

218   period is shown in Figure S2. Very good correlations are observed for every chemical component

219   (0.91<r^2<0.98, n=1402, hourly average) - chloride excluded - with slopes relatively close to one

220   (0.87<slopes<1.42), indicating a fairly good comparability between both instruments. One of the two

221   ACSM also participated in the first-ever inter-ACSM comparison exercise performed between 13

222   different European Q-ACSMs during 3 weeks in Paris, France (Crenn et al., 2015). Satisfactory

223   performances - defined by |z-scores|<2 - are reported for our instrument regarding every chemical

Atmospheric
Chemistry
and Physics
Discussions

224   component and NR-PM$_1$ mass, attesting the consistency of our measurements with other European

225   sites.

226   Measurements performed by the ACSM and independent off-line and on-line analytical

227   techniques are compared in Figure 1 and Table 1. An overall good agreement is found for every major

228   components throughout the year (typically $r^2>0.8$), although discrepancies are observable for specific

229   species and seasons. On the annual scale, a good agreement ($r^2=0.77$, n=317) is found between organics

230   from ACSM and OC from filter measurements in spite of expected filter sampling artefacts (Maimone et

231   al., 2011; Turpin et al., 2000; Watson et al., 2009). Even better agreements are observed on a seasonal

232   basis ($r^2\sim0.9$), with steeper slopes in summer compared with winter, which likely reflects the different

233   degrees of oxygenation of organics among seasons (leading to different OM-to-OC ratios). However,

234   these slopes cannot be directly regarded as the OM-to-OC ratios due to i) differences in size fractions

235   between both methods (PM$_1$ for ACSM and PM$_{2.5}$ for filter measurements) and ii) uncertainties related

236   to RIE$_{Org}$ for ACSM measurements (Budisulistiorini et al., 2014; Ripoll et al., 2015). An estimation of the

237   OM-to-OC ratio for submicron organics applying the methodology described by Canagaratna et al.

238   (2015) is discussed in Sect. 4.2. Good correlations are observed for nitrate during all seasons ($r^2>0.9$) but

239   summer ($r^2=0.5$), which is most likely related to enhanced evaporative losses of ammonium nitrate from

240   filter during the latter season (Chow et al., 2005; Schaap et al., 2004). Slopes range from 0.9 to 1.4 -

241   summer excluded - which is comparable to what is reported elsewhere (Budisulistiorini et al., 2014;

242   Crenn et al., 2015; Ripoll et al., 2015). Very good correlations are observed for sulfate in every season

243   ($r^2=0.9-1.0$) with slopes close to 1 (0.9-1.1, winter excluded), consistent with its presence in the

244   submicronic size fraction and its low volatility leading to the minimization of sampling artefacts. Note

245   that discrepancies have been reported when comparing sulfate measured by the ACSM (Petit et al.,

246   2015) or the AMS (Zhang, 2005) with independent measurements. Our results suggest that ammonium

247   sulfate calibrations should be performed to experimentally determine sulfate RIEs, which appear to be

248   instrument-specific but stable over several months. Although aerosols are slightly acidic on average at

249   the study site, ammonium mostly neutralizes nitrate and sulfate throughout the campaign and thus

250   exhibits behaviour in between the two latter compounds. Higher uncertainties are associated with

251   chloride from filter quantification, resulting in no agreement with ACSM measurements in summer

252   when the concentrations are the lowest ($r^2=0.00$), and fairly good agreement during the other seasons

253   ($r^2=0.64-0.77$). The high slope observed for the ACSM#1 (e.g. 2.1 during spring) compared to the fairly

254   good slopes observed for ACSM#2 (0.7-1.1) suggests that chloride RIE might be instrument-specific and

Atmospheric
Chemistry
and Physics
Discussions

255 require appropriate calibrations for its accurate quantification (see also Riffault et al., 2013 on this

256 topic).

257   The sum of NR-PM$_1$ components and BC has been compared to the volume concentration of

258 PM$_1$. Good agreement is found between both variables (r^2>0.8) giving further confidence on the

259 consistency of our ACSM measurements. The annual average particle density estimated from this

260 comparison (i.e. slope) is 1.6, which is typical of ambient aerosol particles densities (1.5-1.9 in Hand and

261 Kreidenweis, 2002; Hu et al., 2012; McMurry et al., 2002; Pitz et al., 2003, 2008). The higher densities

262 observed during spring and summer (1.9-2.0) than autumn and winter (1.3-1.5) are likely due to the

263 enhanced contribution of secondary aerosol and aged particles during the former period (Pitz et al.,

264 2008).

265

266   3.2. Organic apportionment quality control

267 First, during the aforementioned inter-ACSM comparison study (Crenn et al., 2015), source

268 apportionment of organics was performed based on data from 13 Q-ACSMs (Fröhlich et al., 2015),

269 including one ACSM used in the present study. Satisfactory performances (|z-scores|<2) are reported for

270 our ACSM using a similar approach as adopted in this study. This result demonstrates that our

271 instrument and the associated data treatment, including the source apportionment modelling, are

272 capable of accurately identifying and quantifying OA sources.

273

274   3.2.1.   Model configurations

275   Regarding our specific study, the configuration applied to reach the optimal SA of organics is

276 thoroughly discussed in Sect. S2 (constrained factor profiles, number of factors, *a*-values and

277 integration-period durations). Briefly, constraining both HOA and BBOA factors result in satisfactory

278 solutions with relevant factor profiles, time series and daily cycles. Other configurations (e.g.

279 unconstrained factors) lead to unsatisfactory results with high seed variability, mixing of factors or

280 absence of key fragments in identified profiles (e.g. absence of *m/z* 43 and 44 in BBOA contrary to what

281 is reported in Heringa et al., 2011, Figure S3). Solutions applying different number of factors are

282 investigated. Three-factors (HOA, BBOA and OOA) are retained during spring, autumn and winter

283 whereas two factors (HOA and OOA) are most suitable during summer. A lower number of factors

284 results in a mixing of them, whereas a higher number generates additional factors - e.g. semi-volatile

285 OOA (SV-OOA) during summer, OOA-BBOA during autumn - which are not satisfactory - e.g. missing

286 fragments or poor correlations with external data, see Table S1. BBOA cannot be clearly identified

Atmospheric
Chemistry
and Physics
Discussions

287   during summer i.e. in this season agricultural waste burning contributions are estimated to be minor

288   (maximum 3-4% of OA, Sect. S2). Note that COA could not be evidenced, likely due to the type of site

289   studied (regional background) and the lower sensitivity, time- and mass-to-charge-resolution of the

290   ACSM compared to classical AMS instruments (further discussed in Sect. S2). Uncertainties associated

291   with factor contributions are estimated by performing sensitivity tests on a-values, which are regarded

292   as the most subjective input parameters. Five scenarios putting very low to very high constraints on the

293   reference factor profiles have been defined (see Table S2). Comparable solutions in terms of relative

294   contributions (Figure S4) and agreement with independent measurements (Table S2) are found when

295   applying low to high constraints following the empiric recommendations of Crippa et al. (2014).

296   Unsatisfactory solutions are generally reached under the extreme scenarios (fully fixed factor profiles

297   and m/z specific standard deviations of reference factor profiles). We decided to apply low constraints

298   (i.e. a-values of 0.1 and 0.5 for HOA and BBOA, respectively) to let as much freedom as possible to our

299   factor profiles while remaining in the range of plausible solutions. SA was performed on 3-months, 6-

300   months and 1-year datasets. Although comparable solutions are found for each configuration (number

301   of factors, factor profiles, diurnal cycles, comparisons with external data), applying SA on seasonal

302   datasets was preferred since i) the seasonal variability of factor profiles is captured and ii) questionable

303   results are observed in summer for 6-months and 1-year configurations (see Sect. S2). When comparing

304   the sum of OA factor concentrations and measured OA on the annual scale, OA is very well modelled

305   (r^2=0.97, slope=0.98±0.00, intercept=0.1±0.0 µg/m^3, n=14842).

306

307   3.2.2.   Model optimal solution

308   Factor profiles, contributions and daily cycles of the optimal SA solution are presented in Figure

309   2. Independent factor profiles and time series are found for each season, which is a prerequisite for

310   having reliable SA solutions. HOA is identified during every season and exhibits a profile dominated by

311   alkyl fragments such as m/z 55 (from the $C_nH_{2n-1}^+$ ion series) and m/z 57 (from $C_nH_{2n+1}^+$ ion series; Ng et

312   al., 2011c). Its relative contribution peaks in the morning and is higher during weekdays than weekends,

313   which is characteristic of traffic emissions. BBOA is found during every season but summer and has a

314   profile similar to that of HOA, except for the high contribution of m/z 60 ($C_2H_4O_2^+$) and 73 ($C_3H_5O_2^+$),

315   which have been suggested as biomass burning markers (Lee et al., 2010 and references therein). A

316   distinct daily cycle with higher contributions during night-time than daytime is observed, in addition to

317   higher contributions during weekends than weekdays, consistent with residential heating emissions. The

318   low BBOA concentrations modelled during late spring and early autumn, as well as the small increased

319   contribution observed during the morning also suggest residential heating emissions. OOA is identified

320   thanks to the predominant contribution of m/z 44 (CO_2^+) and 43 ($C_2H_3O^+$). The higher contribution of f_{44}

321   (defined as m/z 44 to total organic signal; 0.17-0.23 depending on seasons) with respect to f_{43} (defined

322   similarly; 0.05-0.09) suggests that this OOA factor is highly oxidized and presents low volatility (LV-)

323   rather than semi-volatility (SV-) OOA characteristics (see Jimenez et al., 2009 and Zhang et al., 2011 for

324   definitions of these components). This statement is supported by very good correlations (r^2=0.96-0.99)

325   found between our unconstrained OOA profiles and the average low-volatility OOA (LV-OOA) profile

326   reported by Ng et al. (2011c) from 6 AMS studies. Interestingly, our OOA profiles present slight seasonal

327   differences that likely reflect changes in source contributions and/or physical-chemical processes in this

328   factor. For instance, f_{60} in OOA profiles is enhanced in winter (0.014) compared with other seasons

329   (0.001-0.004), which suggests that biomass burning contributes to this factor during the aforementioned

330   season, consistent with different studies reporting f_{60} in secondary OA from biomass burning (e.g.

331   Cubison et al., 2011; Heringa et al., 2011; see Sect. S2). Daily cycles are comparable for all seasons with a

332   bimodal pattern characterized by a small peak during night-time and a prominent peak during daytime.

333   The latter peak suggests that a fraction of (LV-) OOA could be locally rather than regionally produced on

334   the time scale of few hours only, likely due to enhanced photochemical activities during daytime. The

335   former peak could be due to i) the condensation of highly oxygenated semi-volatile material favoured by

336   night-time thermodynamic conditions or ii) a contribution of SV-OOA in our OOA factor, which is

337   generally dominated by LV-OOA. The absence of an f_{44} night-time peak (Sect. 4.2) suggests that the

338   second assumption is most probable implying that both SV-OOA and LV-OOA influence our OOA factor.

339

340   3.2.3.   Time series comparisons

341   Comparisons between our OA factors, m/z tracer and independent species time series are

342   shown in Table 2. OOA time series show very good agreement with Org_43 (organic signal at m/z 43)

343   and Org_44 (r^2>0.8 and 0.9, respectively) and relatively good agreement with secondary inorganic

344   species (e.g. $r^2 \geq 0.5$ for ammonium), indicating that this factor can be regarded as a surrogate for

345   secondary organic aerosols. Comparisons with sulfate (a low-volatility species) and nitrate (a semi-

346   volatile species) confirm that our OOA factor might be a mix of SV- and LV-OOA, since better agreement

347   is found with one or the other compound depending on the season studied. BBOA exhibits very good

348   coefficients of determination when compared with its presumable fragment tracers Org_60 and Org_73

349   (r^2>0.97), giving further confidence on its appropriate quantification. Good correlations are generally

350   found between BBOA and BC ($r^2 \geq 0.5$, except for summer) indicating that a large proportion of BC stems

Atmospheric
Chemistry
and Physics
Discussions

351   from biomass burning, consistent with previous findings at the study site (Gilardoni et al., 2011, from EC

352   measurements). A good agreement is also observed with CO ($r^2 \geq 0.7$), as already reported in the Alpine

353   valleys (e.g. Gaeggeler et al., 2008). HOA is not as well correlated with external data or specific m/z,

354   which could be related to i) the absence of clear m/z tracers for this factor due to similarities with BBOA

355   profile, ii) the absence of clear external tracers due to co-emissions by fossil fuel and biomass burning

356   activities of BC, CO and NOx and iii) possible uncertainties associated with the apportionment between

357   HOA and BBOA. The first two assumptions are attested by the better agreement observed between HOA

358   and m/z fragments or independent data during summer (e.g. $r^2=0.52$, n=2208 between HOA and BC) and

359   specific months (e.g. May, September), when biomass burning contributions are negligible. Although

360   uncertainties associated with the accurate apportionment of HOA and BBOA cannot be excluded,

361   several pieces of evidence indicate that a mixing of both factors is unlikely since HOA and BBOA present

362   i) independent factor time series during all seasons ($r^2=0.1-0.2$), ii) distinct and relevant daily cycles and

363   iii) no significant a-value variability attesting their robustness.

364

365   4.   Discussion

366   The meteorological representativeness of this one-year measurement is assessed by comparing the

367   solar irradiation, precipitation, and temperature monthly averages to the ones measured during 1990-

368   2010 at the study site (Figure S5). Comparable seasonal averages are generally found in our study and

369   during the bidecadal reference period. Nevertheless compared to 1990-2010, Spring 2013 was rainier,

370   Summer 2013 slightly warmer and sunnier, and Winter 2013-2014 rainier. Further information regarding

371   the representativeness of measurements performed at the study site during the year 2013 can be found

372   in Putaud et al. (2014a).

373

374   4.1. Chemical composition of NR-PM$_1$

375   An overview of the chemical composition of NR-PM$_1$ retrieved during this campaign is shown in Figure 3.

376   The annual averaged NR-PM$_1$ mass reported here (14.2 µg/m^3) ranges amongst the highest NR-PM$_1$

377   levels reported at rural and urban downwind sites in Europe (Crippa et al., 2014) and worldwide

378   (Jimenez et al., 2009; Zhang et al., 2007, 2011). It is comparable to NR-PM$_1$ levels reported during

379   specific campaigns in the urban areas of New York City (USA, 12 µg/m^3, Weimer et al., 2006), Tokyo

380   (Japan, 12-15 µg/m^3, Takegawa et al., 2006) or Manchester (UK, 14 µg/m^3, Allan et al., 2003a, 2003b).

381   Our annual average NR-PM$_1$ mass is higher than the 10 µg/m^3 guidelines given by the World Health

382   Organization for the annual average PM$_{2.5}$ mass (including refractory and non-refractory compounds;

Atmospheric
Chemistry
and Physics
Discussions

383   WHO, 2006). After similar conclusions have been drawn for $PM_{2.5}$ and PM_{10} size fractions (Putaud et al.,

384   2010), the Po Valley appears to be one of the most polluted regions in Europe with regard to $NR\text{-}PM_1$

385   levels this time. Submicron aerosol particles are mostly made of organics (58%), nitrate (21%), sulfate

386   (12%) and ammonium (8%). The predominance of organics is typical of urban downwind sites (e.g.

387   average of 52% reported in Zhang et al., 2011). On the other hand, the noticeable proportion of nitrate

388   is characteristic of urban sites (18% in Zhang et al., 2011), which likely reflects the substantial influence

389   of anthropogenic activities emissions at our regional site. As a result, sulfate exhibits particularly low

390   contributions at the study site compared with other locations (generally >20% in Zhang et al., 2011).

391   NR-PM_1 levels present a clear seasonality with higher levels during spring (~18 $\mu g/m^3$) and

392   winter (~15 $\mu g/m^3$) compared with summer and autumn (~12 $\mu g/m^3$). Higher levels were expected

393   during cold months due to enhanced biomass burning emissions, lower boundary layer heights (BLH)

394   and previous observations (Putaud et al., 2013). Expected seasonal variations of the chemical

395   composition of $NR\text{-}PM_1$ are observed, with i) higher nitrate contributions during the cold season which

396   favours its partitioning in the condensed phase (Clegg et al., 1998), ii) higher sulfate contributions during

397   summer associated with enhanced photochemical production (Seinfeld and Pandis, 2006), and iii)

398   relatively stable contributions for ammonium (mainly neutralizing the two previous species) and

399   organics (discussed later on).

400   A focus will now be made on daily cycles of the chemical composition of $NR\text{-}PM_1$ (Figure 4),

401   displayed for the first time during the 4 seasons in the Po Valley, thanks to the high time resolution and

402   stability of the ACSM. On the annual scale, daily cycles of $NR\text{-}PM_1$ levels are characterized by

403   significantly higher concentrations during night time than daytime, likely due to lower BLH, higher wood

404   burning emissions (during cold seasons) and lower temperatures favouring the partitioning of semi-

405   volatile inorganic (mainly ammonium nitrate) and organic material in the condensed phase, to name a

406   few. A distinct peak is however observed around noon, probably caused by enhanced photochemical

407   production of secondary inorganic (mostly ammonium sulfate) and organic compounds, especially

408   during summer (Figure S6). Note that this annual daily pattern is the combination of distinct daily cycles

409   varying with the season studied (Figure S6). In terms of relative chemical composition, organics are

410   dominating $NR\text{-}PM_1$ mass independently of the time of the day, with median contributions ranging from

411   ~60 to 70%. Nitrate exhibits higher contribution during night time due to its abovementioned semi-

412   volatile nature. Sulfate shows unexpected daily cycles with significantly different (99.99% confidence

413   level) relative contributions - and absolute concentrations - during daytime (~15% of $NR\text{-}PM_1$ mass

414   around noon) compared to night time (~10% around midnight, Figure 4), although its formation was

415   expected to occur mainly over longer time scales (i.e. days) in cloud droplets (Ervens et al., 2011). This

416   observation could be due to i) local production of sulfate with increased photochemical production

417   around noon at the study site and/or ii) diurnal changes of the atmospheric stratification in the Po Valley

418   as described by Saarikoski et al. (2012), enhancing aged particle contribution during the middle of the

419   day and the afternoon. Non-refractory chloride (mostly NH_4Cl, Huang et al., 2010) exhibits very low

420   contributions independently of the hour of the day (medians below 0.5% of NR-PM_1 mass) with however

421   a slight increase at night, which is likely due to its presumable semi-volatile nature here. Note that 30

422   min averaged chemical composition is also presented in Figure 3, capturing sudden variations of PM_1

423   levels and chemical composition throughout the year, highlighting the velocity at which changes in

424   chemical processes and source emissions occur.

425

426   4.2. Focus on organic aerosols

427   An overview of the contribution of HOA, BBOA and OOA to OA is shown in Figure 5. On the annual

428   average, the organic fraction is dominated by the secondary component (OOA, 66%). Although this OOA

429   contribution is substantial, higher proportions are generally reported at rural and urban downwind sites

430   worldwide (90 and 82% of OA on average, respectively, Zhang et al., 2011). This lower relative

431   contribution of OOA is related to the higher contribution of (primary) BBOA in our study (23% of OA on

432   the annual average) compared to the previous ones. Considerable contributions of BBOA are explained

433   by the specific location of the study site in the vicinity of the Alps, where biomass burning is a major

434   contributor to OA (Belis et al., 2011; Herich et al., 2014; Lanz et al., 2010). Biomass burning emissions

435   hence substantially affect OA levels on the annual scale here. The contribution of HOA is comparatively

436   smaller (11%), indicating that despite the expected large contributions of fossil fuel emissions (i.e. traffic

437   and industrial emissions), those are not the major sources of primary OA at the study site. On the other

438   hand, it is likely that fossil fuel emissions of volatile organic compounds (VOCs) - which are OOA

439   precursors - contribute to our OOA levels as reported elsewhere (Gentner et al., 2012; Volkamer et al.,

440   2006). At the study site, Gilardoni et al. (2011) previously estimated on the basis of ^{14}C analyses that

441   secondary organic carbon stemming from fossil emissions might represent 12% of OC on the annual

442   average. In other words, fossil fuel emissions could represent approximately a quarter (12+11=23%) of

443   total OA mass when both primary and secondary OA fractions are accounted for. The analysis of the

444   components' seasonal variations show relatively stable HOA contributions (9-14%), higher contributions

445   of BBOA during cold seasons due to residential heating (up to 36% of OA on average during winter) and

Atmospheric
Chemistry
and Physics
Discussions

446   higher OOA contributions during summer related to enhanced photochemical production (86% of OA on

447   average).

448   OA can be further characterized investigating specific organic fragments. m/z 44 (mainly CO_2^+)

449   and 43 (mainly $C_2H_3O^+$) signals give insights on the nature of OA, as the former is primarily related to

450   acids or acid-derived species whereas the latter is mostly associated with non-acid oxygenates (Duplissy

451   et al., 2011; Ng et al., 2011b). Daily variations of both f_{44} and f_{43} are shown in Figure 6, along with other

452   major organic fragments. On average, f_{44} is predominant with respect to f_{43} (15 and 7%, respectively),

453   which indicates that acid species dominate the OA composition with respect to non-acid oxygenates.

454   Both fragments present different daily patterns underlying distinct mechanisms of formation. Acids'

455   contributions are enhanced during daytime, which could be explained by photochemical processes

456   and/or daily BLH variations as already discussed for sulfate. Non-acid oxygenates exhibit higher

457   contributions during night time than daytime, although the amplitude of their daily cycles is less

458   pronounced than that of acid species (~1 and 3%, respectively). This pattern could be due to i) the

459   formation of semi-volatile non-acids during night time by e.g. condensation favoured by low

460   temperatures as previously found for semi-volatile OOA (Lanz et al., 2007), ii) their degradation during

461   daytime by e.g. fragmentation reactions (Daumit et al., 2013) and/or iii) their conversion into acid-

462   related species during daytime by e.g. functionalization or oligomerization reactions (Daumit et al.,

463   2013). It should be specified that the enhancement of f_{44} during daytime (~2%) and the decreasing of f_{43}

464   during night-time (~1%) only represent a small fraction of their total contributions to OA (medians of 13-

465   16% and 7-8% depending on the time of the day, respectively, Figure 6), suggesting that most acid and

466   non-acid oxygenates have been formed before reaching our sampling site, i.e. have been imported from

467   other regions. The other major OA fragments (m/z 29, 55, 57 and 60) present i) constant contributions

468   for f_{29} due its various emission sources (HOA, BBOA, OOA; Ng et al., 2011c), ii) the absence of lunch peak

469   for f_{55} (and also for the absolute contributions of m/z 55) consistent with the presumable low influence

470   of cooking emissions, iii) morning and evening peaks for f_{57} characteristics of fossil fuel emissions and iv)

471   higher contributions during night time for f_{60} in agreement with its biomass burning origin.

472   Using f_{43} and f_{44}, the oxygen-to-carbon (O/C), OM-to-OC (OM/OC), hydrogen-to-carbon (H/C)

473   ratios and the carbon oxidation state (OSc) have been estimated for total OA based on the

474   methodologies described by Aiken et al. (2008), Kroll et al. (2011) and Ng et al. (2011b), and applying the

475   parameterization defined in Canagaratna et al. (2015), which can be summarized as follows:

476   O/C= 4.31 f_{44}+ 0.079   (1)

477   OM/OC= 1.28 O/C+ 1.17   (2)

Atmospheric
Chemistry
and Physics

Discussions

Open Access

EGU

478    $H/C = 1.12 + 6.74\,f_{43} - 17.77\,f_{43}^2$ (3)

479    $OSc = 2*O/C - H/C$ (4)

480   with H/C (and therefore OSc) being estimated only if $f_{44} > 0.05$ and $f_{43} > 0.04$ (Canagaratna et al., 2015).

481   The errors (average absolute value of the relative error) are estimated to be 28%, 8% and 13% for O/C,

482   OM/OC and H/C for standard molecules, respectively, and 0.06 units for OSc (Canagaratna et al., 2015).

483   Discrepancies in f_{44} quantifications between different ACSMs, and between ACSMs and AMS (Crenn et

484   al., 2015; Fröhlich et al., 2015) are however likely to increase the uncertainties associated with O/C,

485   OM/OC and OSc estimates. In particular, in the abovementioned inter-instrument comparison, ACSMs

486   have been reported to overestimate f_{44} by up to a factor of 2 compared to the HR-ToF-AMS (Fröhlich et

487   al., 2015). Comparisons with studies using (HR-ToF-) AMS instruments will thus not be reported and only

488   variations within this dataset will be discussed. Regarding the two ACSMs used in this study, absolute

489   differences between median estimates from two-months co-located measurements in summer are 0.05,

490   0.07, 0.07 and 0.17 for O/C, OM/OC, H/C and OSc, respectively (see Figure S7). Seasonal and annual O/C,

491   OM/OC, H/C and OSc are shown in Figure 7. High O/C, OM/OC and OSc are found on the annual scale

492   (medians of 0.7, 2.1 and -0.2, respectively), reflecting once more the aged, oxidized properties of

493   organic matter at the study site, consistent with the predominance of the OOA component. Little

494   seasonal variations are observed for the aforementioned variables hence highlighting the high degree of

495   oxidation of OA throughout the year (Figure 7). The unexpectedly high degree of oxygenation of OA

496   observed during cold seasons despite the increased contribution of primary BBOA (with OM/OC ratios of

497   1.4-1.6) could be explained by the contribution of secondary BBOA in our OOA factor during these cold

498   seasons, which could be associated with the enhancement of e.g. dicarboxylic and ketocarboxylic acid

499   contents (Kundu et al., 2010) that have extremely high OM/OC ratios (up to 3.8 and 3.1, respectively,

500   Turpin and Lim, 2001). This assumption is supported by the higher proportion of f_{60} in our OOA factor

501   (discussed in Sect. 3.2 and S2), as well as the surprisingly high OM/OC ratio observed for OOA during

502   winter (2.5 compared to 2.2-2.4 during the other seasons). Note that Canonaco et al. (2015) also report

503   a higher f_{44} in (LV-) OOA in winter compared to summer in Zurich (Switzerland). According to these

504   authors, this could be due to enhanced aqueous-phase production of (LV-) OOA in clouds or hygroscopic

505   aerosols in winter, which would lead to higher levels of oxygenation compared to gas-phase oxidation

506   mechanisms typically occurring during summer.

507

508   4.3. Possible implications for PM abatement strategies

Atmospheric
Chemistry
and Physics
Discussions

509   In order to investigate the characteristics of fine aerosol pollution events, the variations of NR-PM$_1$

510   chemical composition and OA factors' contributions as a function of total NR-PM$_1$ mass are examined

511   (Figure 8). Distinct trends are observed depending on the chemical species and OA components studied.

512   The proportion of nitrate is clearly enhanced with increasing NR-PM$_1$ levels (from ~10 to >30% when

513   [NR-PM$_1$]>30 µg/m^3) indicating that nitrate - or NO$_x$ - abatement policies should be highly effective when

514   attempting to limit PM$_1$ pollution events in the Upper Po Valley. Sulfate shows an opposite trend with

515   decreasing relative contribution when NR-PM$_1$ mass increases (e.g. <5% when [NR-PM$_1$]> 50 µg/m^3),

516   likely due to the lower concentrations of sulfate during cold seasons, when the highest number of

517   pollution events is observed. The proportion of organics is substantial (48-66%) independently of NR-

518   PM$_1$ mass, justifying once again the importance of determining its sources to design adequate

519   abatement policies. When focusing on the organic fraction, BBOA is the only OA factor exhibiting

520   increased contributions (from ~10 to >40%) with increased NR-PM$_1$ mass (from <10 to >60 µg/m^3),

521   which points out the PM abatement potential of effective biomass burning emission reductions. HOA

522   levels are rather constant throughout the year and therefore their proportions steadily decrease when

523   NR-PM$_1$ levels increase, implying that local fossil fuel related emissions of primary OC are not the main

524   responsible for submicron pollution events observed at the study site. Although OOA always represents

525   a major fraction of OA (41-75% depending on the mass bin studied), its contribution steadily decreases

526   with increasing NR-PM$_1$ mass. This unexpected result signifies that even though aged, secondary,

527   oxidised organics are the main contributor to OA on the annual average (66%), they do not play a

528   prominent role in fine PM acute pollution events.

529   Current European legislations set daily and/or annual PM limit values depending on the size fraction

530   addressed (Directive 2008/50/EC). Volume size distributions suggest that approximately 90% of the

531   PM$_{2.5}$ mass concentration is borne by particles below an aerodynamic diameter of 1 µm at the study site

532   (Putaud et al., 2014a). Therefore, measures tackling the main constituents of the submicron aerosol

533   fraction would be efficient for complying with PM$_{2.5}$ legislations. Based on the chemical characterization

534   of NR-PM$_1$ and SA of its organic fraction with a time-resolution of 30 min over 1-year, this study provides

535   new evidence which could orient PM abatement strategies also at similar regional background sites of

536   the Po Valley. On the annual scale, OA and especially OOA should be of main concern given their

537   predominance in NR-PM$_1$ chemical composition (Figure 3). On the seasonal scale, efforts should be

538   directed towards the cold seasons (winter and early spring), for which the highest NR-PM$_1$ levels are

539   observed, due to specific meteorological conditions (e.g. low BLH, low temperatures) and emission

540   sources (e.g. biomass burning, Figure 3 and Figure 5). In particular, measures addressing emissions of

Atmospheric
Chemistry
and Physics
Discussions

541   NO_x and BBOA would be the most efficient for reducing the magnitude and frequency of PM pollution

542   events (Figure 8).

543   Recommendations for PM abatement strategies are formulated here from a legislative perspective,

544   which aims at decreasing PM levels. Although diminishing PM levels should help reducing PM impacts,

545   the existence of a direct causal relationship can be debatable since each chemical component has a

546   specific effect on human health (WHO, 2013), the radiative forcing (Boucher et al., 2013) or ecosystems

547   (e.g. Carslaw et al., 2010). For instance, implementing policies aiming at mitigating nitrate

548   concentrations - as suggested previously in this section - would likely have limited health benefits

549   according to toxicological studies (Reiss et al., 2007; Schlesinger and Cassee, 2003), and should lead to

550   an increased global warming (Boucher et al., 2013). On the other hand, measures reducing BBOA levels

551   should be beneficial, since the cardio-vascular effects of biomass burning particles have been widely

552   reported in the literature (Bølling et al., 2009; Miljevic et al., 2010; Naeher et al., 2007) and could be

553   similar to those of traffic-emitted particles (WHO, 2013 and references therein), whereas their impacts

554   on the radiative forcing could be null (Boucher et al., 2013). Strategies aiming at reducing solely PM

555   mass are therefore limited, and an assessment of their impacts - e.g. using integrated assessment

556   models (Carnevale et al., 2012; Janssen et al., 2009) with appropriate parameterizations of fundamental

557   processes - would be beneficial.

558

559   5.   Conclusion and perspectives

560   The NR-PM_1 chemical composition and the apportionment of the organic fraction have been

561   investigated for the first time with this completeness at a regional background site of the Po valley

562   (Italy), using high time-resolution (30 min) and long term (1 year) measurements with a state-of-the-art

563   quality assured ACSM and the most advanced factor analysis methods. Comparisons between two

564   ACSMs show very good time series correlations for the major compounds ($0.91<r^2<0.98$, n=1402) with

565   however discrepancies in their absolute concentrations (0.9<slopes<1.4). These results are promising

566   with regard to the consistency of ACSM measurements at different locations, but also underlines the

567   importance of conducting inter-ACSM comparisons to define common protocols and assure data

568   comparability among the European ACSM network (see Crenn et al., 2015). Comparisons between ACSM

569   and independent analytical technique measurements show an overall good agreement for major

570   components throughout the year (typically $r^2>0.8$). Discrepancies observed in time series correlations

571   and quantifications (i.e. slopes) for specific species and seasons (e.g. nitrate in summer) are attributed

572   to filter sampling artefacts. These results are encouraging regarding the potential implementation of

18

573   ACSMs in air quality networks as a replacement of traditional filter-based techniques, to measure the

574   artefact-free chemical composition of fine aerosols with high time-resolution. Additional comparison

575   studies are nevertheless needed to support our results, and further technical development allowing the

576   refractory carbon fraction to be accounted for is required.

577   NR-PM$_1$ and PM$_1$ levels measured in the upper Po Valley (14.2 and 15.3 µg/m^3 on the annual

578   average, respectively) are among the highest reported in Europe, stressing the need for implementing

579   effective PM abatement strategies in this region. On average, the chemical composition of non-

580   refractory submicron aerosol is dominated by organic aerosol (58% of NR-PM$_1$), which is composed of

581   HOA (11% of OA), BBOA (23%) and OOA (66%). Fossil fuel combustion is thus not a major source of

582   primary OA in this area of the Po Valley. Primary BBOA significantly contributes to OA on the annual

583   average and especially during winter (36%). Our OOA component is highly oxidised and aged with an LV-

584   OOA spectral signature, a large proportion of acid-related species and high OM/OC ratios. Highly

585   oxidised OA properties are observed during all seasons, surprisingly including winter, which could reflect

586   secondary BBOA influence and OOA aqueous-phase formation processes during cold seasons. Further

587   research aiming at identifying the sources of OOA - including secondary BBOA using e.g. high resolution

588   mass spectrometric techniques (Crippa et al., 2013) or proton nuclear magnetic resonance (Paglione et

589   al., 2014) - and better estimating O/C, OM/OC and OSc parameters would be beneficial.

590   Specific recommendations for PM abatement strategies at a regional level can be suggested.

591   The higher frequency of particulate pollution peaks observed during cold seasons suggests an

592   orientation of future policies towards these periods. BBOA and nitrate present increasing relative

593   contributions with increasing fine aerosol levels, which suggests that wood burning and NO$_x$ emission

594   reductions should notably decrease NR-PM$_1$ pollution events. Note that these recommendations are

595   only formulated in the perspective of reducing PM levels, assuming a subsequent reduction of PM

596   impacts. Additional dimensions - e.g. specific impacts of each chemical component, short versus long-

597   term exposure, co-benefit of sanitary and climatic impacts - should also be considered when defining

598   PM abatement strategies. In a broader context, the use of high time resolution analytical techniques for

599   the measurement of PM pollution properties can help better shape our future air quality policies.

600

Atmospheric
Chemistry
and Physics
Discussions

607 **References**

608

609 Aerodyne: Aerosol Chemical Speciation Monitor: Data Acquisition Software Manual, available at:
610   ftp://ftp.aerodyne.com/ACSM/ACSM_Manuals/ACSM_DAQ_Manual.pdf (last access: 15
611   February 2016), 2010a.
612 Aerodyne: Aerosol Chemical Speciation Monitor: Data Analysis Software Manual, available at:
613   ftp://ftp.aerodyne.com/ACSM/ACSM_Manuals/ACSM_Igor_Manual.pdf (last access: 15
614   February 2016), 2010b.
615 Aiken, A. C., DeCarlo, P. F., Kroll, J. H., Worsnop, D. R., Huffman, J. A., Docherty, K. S., Ulbrich, I. M.,
616   Mohr, C., Kimmel, J. R., Sueper, D., Sun, Y., Zhang, Q., Trimborn, A., Northway, M., Ziemann, P.
617   J., Canagaratna, M. R., Onasch, T. B., Alfarra, M. R., Prevot, A. S. H., Dommen, J., Duplissy, J.,
618   Metzger, A., Baltensperger, U., and Jimenez, J. L.: O/C and OM/OC ratios of primary, secondary,
619   and ambient organic aerosols with high-resolution time-of-flight aerosol mass spectrometry,
620   Environ. Sci. Technol., 42(12), 4478–4485, doi:10.1021/es703009q, 2008.
621 Allan, J. D., Jimenez, J. L., Williams, P. I., Alfarra, M. R., Bower, K. N., Jayne, J. T., Coe, H., and Worsnop,
622   D. R.: Quantitative sampling using an Aerodyne aerosol mass spectrometer 1. Techniques of
623   data interpretation and error analysis, J. Geophys. Res.-Atmos., 108(D3), 4090,
624   doi:10.1029/2002JD002358, 2003a.
625 Allan, J. D., Alfarra, M. R., Bower, K. N., Williams, P. I., Gallagher, M. W., Jimenez, J. L., McDonald, A. G.,
626   Nemitz, E., Canagaratna, M. R., Jayne, J. T., Coe, H., and Worsnop, D. R.: Quantitative sampling
627   using an Aerodyne aerosol mass spectrometer 2. Measurements of fine particulate chemical
628   composition in two U.K. cities, J. Geophys. Res.-Atmos., 108(D3), 4091,
629   doi:10.1029/2002JD002359, 2003b.
630 Amato, F., Pandolfi, M., Escrig, A., Querol, X., Alastuey, A., Pey, J., Perez, N., and Hopke, P. K.:
631   Quantifying road dust resuspension in urban environment by Multilinear Engine: a comparison
632   with PMF2, Atmos. Environ., 43(17), 2770–2780, doi:10.1016/j.atmosenv.2009.02.039, 2009.
633 Belis, C. A., Cancelinha, J., Duane, M., Forcina, V., Pedroni, V., Passarella, R., Tanet, G., Douglas, K.,
634   Piazzalunga, A., Bolzacchini, E., Sangiorgi, G., Perrone, M.-G., Ferrero, L., Fermo, P., and Larsen,
635   B. R.: Sources for PM air pollution in the Po Plain, Italy: I. Critical comparison of methods for
636   estimating biomass burning contributions to benzo(a)pyrene, Atmos. Environ., 45(39), 7266–
637   7275, doi:10.1016/j.atmosenv.2011.08.061, 2011.
638 Belis, C. A., Karagulian, F., Larsen, B. R., and Hopke, P. K.: Critical review and meta-analysis of ambient
639   particulate matter source apportionment using receptor models in Europe, Atmos. Environ., 69,
640   94–108, doi:10.1016/j.atmosenv.2012.11.009, 2013.
641 Bølling, A. K., Pagels, J., Yttri, K., Barregard, L., Sallsten, G., Schwarze, P. E., and Boman, C.: Health effects
642   of residential wood smoke particles: the importance of combustion conditions and
643   physicochemical particle properties, Part. Fibre Toxicol., 6(1), 29, doi:10.1186/1743-8977-6-29,
644   2009.
645 Boucher, O., Randall, D., Artaxo, P., Bretherton, C., Feingold, G., Forster, P., Kerminen, V.-M., Kondo, Y.,
646   Liao, H., Lohmann, U., Rasch, P., Satheesh, S. K., Sherwood, S., Stevens, B., and Zhang, X.: Clouds
647   and aerosols, in Climate Change 2013: The Physical Science Basis. Contribution of Working
648   Group I to the Fifth Assessment Report of the Intergovernmental Panel on Climate Change,
649   edited by: Stocker, T. F., Qin, D., Plattner, G.-K., Tignor, M., Allen, S. K., Boschung, J., Nauels,
650   A., Xia, Y., Bex, V., and Midgley, P. M., Cambridge University Press, Cambridge, United Kingdom
651   and New York, NY, USA, 2013.
652 Budisulistiorini, S. H., Canagaratna, M. R., Croteau, P. L., Marth, W. J., Baumann, K., Edgerton, E. S.,
653   Shaw, S. L., Knipping, E. M., Worsnop, D. R., Jayne, J. T., Gold, A., and Surratt, J. D.: Real-time

Atmospheric
Chemistry
and Physics
Discussions

654   continuous characterization of secondary organic aerosol derived from isoprene epoxydiols in
655   downtown Atlanta, Georgia, using the Aerodyne aerosol chemical speciation monitor, Environ.
656   Sci. Technol., 47(11), 5686–5694, doi:10.1021/es400023n, 2013.
657 Budisulistiorini, S. H., Canagaratna, M. R., Croteau, P. L., Baumann, K., Edgerton, E. S., Kollman, M. S., Ng,
658   N. L., Verma, V., Shaw, S. L., Knipping, E. M., Worsnop, D. R., Jayne, J. T., Weber, R. J., and
659   Surratt, J. D.: Intercomparison of an aerosol chemical speciation monitor (ACSM) with ambient
660   fine aerosol measurements in downtown Atlanta, Georgia, Atmos. Meas. Tech., 7(7), 1929–
661   1941, doi:10.5194/amt-7-1929-2014, 2014.
662 Canagaratna, M. R., Jayne, J. T., Jimenez, J. L., Allan, J. D., Alfarra, M. R., Zhang, Q., Onasch, T. B.,
663   Drewnick, F., Coe, H., Middlebrook, A., Delia, A., Williams, L. R., Trimborn, A. M., Northway, M.
664   J., DeCarlo, P. F., Kolb, C. E., Davidovits, P., and Worsnop, D. R.: Chemical and microphysical
665   characterization of ambient aerosols with the Aerodyne aerosol mass spectrometer, Mass
666   Spectrom. Rev., 26(2), 185–222, doi:10.1002/mas.20115, 2007.
667 Canagaratna, M. R., Jimenez, J. L., Kroll, J. H., Chen, Q., Kessler, S. H., Massoli, P., Hildebrandt Ruiz, L.,
668   Fortner, E., Williams, L. R., Wilson, K. R., Surratt, J. D., Donahue, N. M., Jayne, J. T., and Worsnop,
669   D. R.: Elemental ratio measurements of organic compounds using aerosol mass spectrometry:
670   characterization, improved calibration, and implications, Atmos. Chem. Phys., 15, 253–272,
671   doi:10.5194/acp-15-253-2015, 2015.
672 Canonaco, F., Crippa, M., Slowik, J. G., Baltensperger, U., and Prévôt, A. S. H.: SoFi, an IGOR-based
673   interface for the efficient use of the generalized multilinear engine (ME-2) for the source
674   apportionment: ME-2 application to aerosol mass spectrometer data, Atmos. Meas. Tech.,
675   6(12), 3649–3661, doi:10.5194/amt-6-3649-2013, 2013.
676 Canonaco, F., Slowik, J. G., Baltensperger, U., and Prévôt, A. S. H.: Seasonal differences in oxygenated
677   organic aerosol composition: implications for emissions sources and factor analysis, Atmos.
678   Chem. Phys., 15(12), 6993–7002, doi:10.5194/acp-15-6993-2015, 2015.
679 Carbone, C., Decesari, S., Paglione, M., Giulianelli, L., Rinaldi, M., Marinoni, A., Cristofanelli, P.,
680   Didiodato, A., Bonasoni, P., Fuzzi, S., and Facchini, M. C.: 3-year chemical composition of free
681   tropospheric PM_1 at the Mt. Cimone GAW global station – South Europe – 2165 m a.s.l., Atmos.
682   Environ., 87, 218–227, doi:10.1016/j.atmosenv.2014.01.048, 2014.
683 Carnevale, C., Finzi, G., Pisoni, E., Volta, M., Guariso, G., Gianfreda, R., Maffeis, G., Thunis, P., White, L.,
684   and Triacchini, G.: An integrated assessment tool to define effective air quality policies at
685   regional scale, Environ. Modell. Softw., 38, 306–315, doi:10.1016/j.envsoft.2012.07.004, 2012.
686 Carslaw, K. S., Boucher, O., Spracklen, D. V., Mann, G. W., Rae, J. G. L., Woodward, S., and Kulmala, M.: A
687   review of natural aerosol interactions and feedbacks within the Earth system, Atmos. Chem.
688   Phys., 10(4), 1701–1737, 2010.
689 Cavalli, F., Viana, M., Yttri, K. E., Genberg, J., and Putaud, J. P.: Toward a standardised thermal-optical
690   protocol for measuring atmospheric organic and elemental carbon: the EUSAAR protocol,
691   Atmos. Meas. Tech., 3, 79–89, 2010.
692 Chow, J. C., Watson, J. G., Lowenthal, D. H., and Magliano, K. L.: Loss of $PM_{2.5}$ nitrate from filter samples
693   in central California, J. Air Waste Manage. Assoc., 55(8), 1158–1168,
694   doi:10.1080/10473289.2005.10464704, 2005.
695 Clegg, S. L., Brimblecombe, P., and Wexler, A. S.: Thermodynamic model of the system $H^+–NH_4^+–SO_4^{2-}$
696    $–NO_3^-–H_2O$ at tropospheric temperatures, J. Phys. Chem. A, 102(12), 2137–2154,
697   doi:10.1021/jp973042r, 1998.
698 Clerici, M. and Mélin, F.: Aerosol direct radiative effect in the Po Valley region derived from AERONET
699   measurements, Atmos. Chem. Phys., 8(16), 4925–4946, 2008.
700 Crawford, J., Cohen, D., Dyer, L., and Zahorowski, W.: Receptor modelling with PMF2 and ME2 using
701   aerosol data from Hong Kong, Australian Nuclear Science and Technology Organisation (ANSTO),

Atmospheric
Chemistry
and Physics
Discussions

702   available at: http://apo.ansto.gov.au/dspace/bitstream/10238/201/1/ANSTO-E-756.pdf (last
703   access: 15 February 2016), 2005.
704 Crenn, V., Sciare, J., Croteau, P. L., Verlhac, S., Fröhlich, R., Belis, C. A., Aas, W., Äijälä, M., Alastuey, A.,
705   Artiñano, B., Baisnée, D., Bonnaire, N., Bressi, M., Canagaratna, M., Canonaco, F., Carbone, C.,
706   Cavalli, F., Coz, E., Cubison, M. J., Esser-Gietl, J. K., Green, D. C., Gros, V., Heikkinen, L.,
707   Herrmann, H., Lunder, C., Minguillón, M. C., Močnik, G., O'Dowd, C. D., Ovadnevaite, J., Petit, J.-
708   E., Petralia, E., Poulain, L., Priestman, M., Riffault, V., Ripoll, A., Sarda-Estève, R., Slowik, J. G.,
709   Setyan, A., Wiedensohler, A., Baltensperger, U., Prévôt, A. S. H., Jayne, J. T., and Favez, O.:
710   ACTRIS ACSM intercomparison – part 1: reproducibility of concentration and fragment results
711   from 13 individual quadrupole aerosol chemical speciation monitors (Q-ACSM) and consistency
712   with co-located instruments, Atmos. Meas. Tech., 8(12), 5063–5087, doi:10.5194/amt-8-5063-
713   2015, 2015.
714 Crippa, M., DeCarlo, P. F., Slowik, J. G., Mohr, C., Heringa, M. F., Chirico, R., Poulain, L., Freutel, F., Sciare,
715   J., Cozic, J., Di Marco, C. F., Elsasser, M., Nicolas, J. B., Marchand, N., Abidi, E., Wiedensohler, A.,
716   Drewnick, F., Schneider, J., Borrmann, S., Nemitz, E., Zimmermann, R., Jaffrezo, J.-L., Prévôt, A. S.
717   H., and Baltensperger, U.: Wintertime aerosol chemical composition and source apportionment
718   of the organic fraction in the metropolitan area of Paris, Atmos. Chem. Phys., 13(2), 961–981,
719   doi:10.5194/acp-13-961-2013, 2013.
720 Crippa, M., Canonaco, F., Lanz, V. A., Äijälä, M., Allan, J. D., Carbone, S., Capes, G., Ceburnis, D.,
721   Dall'Osto, M., Day, D. A., DeCarlo, P. F., Ehn, M., Eriksson, A., Freney, E., Hildebrandt Ruiz, L.,
722   Hillamo, R., Jimenez, J. L., Junninen, H., Kiendler-Scharr, A., Kortelainen, A.-M., Kulmala, M.,
723   Laaksonen, A., Mensah, A. A., Mohr, C., Nemitz, E., O'Dowd, C., Ovadnevaite, J., Pandis, S. N.,
724   Petäjä, T., Poulain, L., Saarikoski, S., Sellegri, K., Swietlicki, E., Tiitta, P., Worsnop, D. R.,
725   Baltensperger, U., and Prévôt, A. S. H.: Organic aerosol components derived from 25 AMS data
726   sets across Europe using a consistent ME-2 based source apportionment approach, Atmos.
727   Chem. Phys., 14(12), 6159–6176, doi:10.5194/acp-14-6159-2014, 2014.
728 Cubison, M. J., Ortega, A. M., Hayes, P. L., Farmer, D. K., Day, D., Lechner, M. J., Brune, W. H., Apel, E.,
729   Diskin, G. S., Fisher, J. A., Fuelberg, H. E., Hecobian, A., Knapp, D. J., Mikoviny, T., Riemer, D.,
730   Sachse, G. W., Sessions, W., Weber, R. J., Weinheimer, A. J., Wisthaler, A., and Jimenez, J. L.:
731   Effects of aging on organic aerosol from open biomass burning smoke in aircraft and laboratory
732   studies, Atmos. Chem. Phys., 11(23), 12049–12064, doi:10.5194/acp-11-12049-2011, 2011.
733 Daumit, K. E., Kessler, S. H., and Kroll, J. H.: Average chemical properties and potential formation
734   pathways of highly oxidized organic aerosol, Faraday Discuss., 165, 181,
735   doi:10.1039/c3fd00045a, 2013.
736 Decesari, S., Allan, J., Plass-Duelmer, C., Williams, B. J., Paglione, M., Facchini, M. C., O'Dowd, C.,
737   Harrison, R. M., Gietl, J. K., Coe, H., Giulianelli, L., Gobbi, G. P., Lanconelli, C., Carbone, C.,
738   Worsnop, D., Lambe, A. T., Ahern, A. T., Moretti, F., Tagliavini, E., Elste, T., Gilge, S., Zhang, Y.,
739   and Dall'Osto, M.: Measurements of the aerosol chemical composition and mixing state in the
740   Po Valley using multiple spectroscopic techniques, Atmos. Chem. Phys., 14, 12109–12132,
741   doi:10.5194/acp-14-12109-2014, 2014.
742 Duplissy, J., DeCarlo, P. F., Dommen, J., Alfarra, M. R., Metzger, A., Barmpadimos, I., Prevot, A. S. H.,
743   Weingartner, E., Tritscher, T., Gysel, M., Aiken, A. C., Jimenez, J. L., Canagaratna, M. R.,
744   Worsnop, D. R., Collins, D. R., Tomlinson, J., and Baltensperger, U.: Relating hygroscopicity and
745   composition of organic aerosol particulate matter, Atmos. Chem. Phys., 11(3), 1155–1165,
746   doi:10.5194/acp-11-1155-2011, 2011.
747 EC: Commission of the European communities, Commission staff working paper, Annex to the
748   communication on thematic strategy on air pollution and the directive on "Ambient air quality
749   and cleaner air for Europe", Impact assessment, SEC (2005) 1133, available at:

Atmospheric
Chemistry
and Physics
Discussions

Open Access

750   http://ec.europa.eu/environment/archives/cafe/pdf/ia_report_en050921_final.pdf (last access:
751   15 February 2016), 2005.
752 EEA: Air quality in Europe - 2013 report, European Environment Agency (EEA), report no 9/2013,
753   publication, available at: http://www.eea.europa.eu/publications/air-quality-in-europe-2013
754   (last access: 15 February 2016), 2013.
755 Ervens, B., Turpin, B. J., and Weber, R. J.: Secondary organic aerosol formation in cloud droplets and
756   aqueous particles (aqSOA): a review of laboratory, field and model studies, Atmos. Chem. Phys.,
757   11(21), 11069–11102, doi:10.5194/acp-11-11069-2011, 2011.
758 Ferrero, L., Castelli, M., Ferrini, B. S., Moscatelli, M., Perrone, M. G., Sangiorgi, G., D'Angelo, L., Rovelli,
759   G., Moroni, B., Scardazza, F., Močnik, G., Bolzacchini, E., Petitta, M., and Cappelletti, D.: Impact
760   of black carbon aerosol over Italian basin valleys: high-resolution measurements along vertical
761   profiles, radiative forcing and heating rate, Atmos. Chem. Phys., 14(18), 9641–9664,
762   doi:10.5194/acp-14-9641-2014, 2014.
763 Fröhlich, R., Crenn, V., Setyan, A., Belis, C. A., Canonaco, F., Favez, O., Riffault, V., Slowik, J. G., Aas, W.,
764   Aijälä, M., Alastuey, A., Artiñano, B., Bonnaire, N., Bozzetti, C., Bressi, M., Carbone, C., Coz, E.,
765   Croteau, P. L., Cubison, M. J., Esser-Gietl, J. K., Green, D. C., Gros, V., Heikkinen, L., Herrmann, H.,
766   Jayne, J. T., Lunder, C. R., Minguillón, M. C., Močnik, G., O'Dowd, C. D., Ovadnevaite, J., Petralia,
767   E., Poulain, L., Priestman, M., Ripoll, A., Sarda-Estève, R., Wiedensohler, A., Baltensperger, U.,
768   Sciare, J., and Prévôt, A. S. H.: ACTRIS ACSM intercomparison – part 2: intercomparison of ME-2
769   organic source apportionment results from 15 individual, co-located aerosol mass
770   spectrometers, Atmos. Meas. Tech., 8(6), 2555–2576, doi:10.5194/amt-8-2555-2015, 2015.
771 Gaeggeler, K., Prevot, A. S. H., Dommen, J., Legreid, G., Reimann, S., and Baltensperger, U.: Residential
772   wood burning in an Alpine valley as a source for oxygenated volatile organic compounds,
773   hydrocarbons and organic acids, Atmos. Environ., 42(35), 8278–8287,
774   doi:10.1016/j.atmosenv.2008.07.038, 2008.
775 Gentner, D. R., Isaacman, G., Worton, D. R., Chan, A. W. H., Dallmann, T. R., Davis, L., Liu, S., Day, D. A.,
776   Russell, L. M., Wilson, K. R., Weber, R., Guha, A., Harley, R. A., and Goldstein, A. H.: Elucidating
777   secondary organic aerosol from diesel and gasoline vehicles through detailed characterization of
778   organic carbon emissions, Proc. Natl. Acad. Sci. USA, 109(45), 18318–18323,
779   doi:10.1073/pnas.1212272109, 2012.
780 Gilardoni, S., Vignati, E., Cavalli, F., Putaud, J. P., Larsen, B. R., Karl, M., Stenström, K., Genberg, J.,
781   Henne, S., and Dentener, F.: Better constraints on sources of carbonaceous aerosols using a
782   combined ^{14}C – macro tracer analysis in a European rural background site, Atmos. Chem. Phys.,
783   11(12), 5685–5700, doi:10.5194/acp-11-5685-2011, 2011.
784 Hand, J. L. and Kreidenweis, S. M.: A new method for retrieving particle refractive index and effective
785   density from aerosol size distribution data, Aerosol Sci. Tech., 36(10), 1012–1026,
786   doi:10.1080/02786820290092276, 2002.
787 Herich, H., Gianini, M. F. D., Piot, C., Močnik, G., Jaffrezo, J.-L., Besombes, J.-L., Prévôt, A. S. H., and
788   Hueglin, C.: Overview of the impact of wood burning emissions on carbonaceous aerosols and
789   PM in large parts of the Alpine region, Atmos. Environ., 89, 64–75,
790   doi:10.1016/j.atmosenv.2014.02.008, 2014.
791 Heringa, M. F., DeCarlo, P. F., Chirico, R., Tritscher, T., Dommen, J., Weingartner, E., Richter, R., Wehrle,
792   G., Prévôt, A. S. H., and Baltensperger, U.: Investigations of primary and secondary particulate
793   matter of different wood combustion appliances with a high-resolution time-of-flight aerosol
794   mass spectrometer, Atmos. Chem. Phys., 11(12), 5945–5957, doi:10.5194/acp-11-5945-2011,
795   2011.
796 Hu, M., Peng, J., Sun, K., Yue, D., Guo, S., Wiedensohler, A., and Wu, Z.: Estimation of size-resolved
797   ambient particle density based on the measurement of aerosol number, mass, and chemical size

Atmospheric
Chemistry
and Physics
Discussions

798   distributions in the winter in Beijing, Environ. Sci. Technol., 120830075118007,
799   doi:10.1021/es204073t, 2012.
800 Huang, X.-F., He, L.-Y., Hu, M., Canagaratna, M. R., Sun, Y., Zhang, Q., Zhu, T., Xue, L., Zeng, L.-W., Liu, X.-
801   G., Zhang, Y.-H., Jayne, J. T., Ng, N. L., and Worsnop, D. R.: Highly time-resolved chemical
802   characterization of atmospheric submicron particles during 2008 Beijing Olympic Games using
803   an aerodyne high-resolution aerosol mass spectrometer, Atmos. Chem. Phys., 10(18), 8933–
804   8945, doi:10.5194/acp-10-8933-2010, 2010.
805 Janssen, S., Ewert, F., Li, H., Athanasiadis, I. N., Wien, J. J. F., Thérond, O., Knapen, M. J. R., Bezlepkina, I.,
806   Alkan-Olsson, J., Rizzoli, A. E., Belhouchette, H., Svensson, M., and van Ittersum, M. K.: Defining
807   assessment projects and scenarios for policy support: use of ontology in integrated assessment
808   and modelling, Environ. Modell. Softw., 24(12), 1491–1500, doi:10.1016/j.envsoft.2009.04.009,
809   2009.
810 Jayne, J. T., Leard, D. C., Zhang, X., Davidovits, P., Smith, K. A., Kolb, C. E., and Worsnop, D. R.:
811   Development of an aerosol mass spectrometer for size and composition analysis of submicron
812   particles, Aerosol Sci. Tech., 33(1-2), 49–70, 2000.
813 Jimenez, J. L., Canagaratna, M. R., Donahue, N. M., Prevot, A. S. H., Zhang, Q., Kroll, J. H., DeCarlo, P. F.,
814   Allan, J. D., Coe, H., Ng, N. L., Aiken, A. C., Docherty, K. S., Ulbrich, I. M., Grieshop, A. P.,
815   Robinson, A. L., Duplissy, J., Smith, J. D., Wilson, K. R., Lanz, V. A., Hueglin, C., Sun, Y. L., Tian, J.,
816   Laaksonen, A., Raatikainen, T., Rautiainen, J., Vaattovaara, P., Ehn, M., Kulmala, M., Tomlinson,
817   J. M., Collins, D. R., Cubison, M. J., Dunlea, J., Huffman, J. A., Onasch, T. B., Alfarra, M. R.,
818   Williams, P. I., Bower, K., Kondo, Y., Schneider, J., Drewnick, F., Borrmann, S., Weimer, S.,
819   Demerjian, K., Salcedo, D., Cottrell, L., Griffin, R., Takami, A., Miyoshi, T., Hatakeyama, S.,
820   Shimono, A., Sun, J. Y., Zhang, Y. M., Dzepina, K., Kimmel, J. R., Sueper, D., Jayne, J. T., Herndon,
821   S. C., Trimborn, A. M., Williams, L. R., Wood, E. C., Middlebrook, A. M., Kolb, C. E., Baltensperger,
822   U., and Worsnop, D. R.: Evolution of organic aerosols in the atmosphere, Science, 326(5959),
823   1525–1529, doi:10.1126/science.1180353, 2009.
824 Kroll, J. H., Donahue, N. M., Jimenez, J. L., Kessler, S. H., Canagaratna, M. R., Wilson, K. R., Altieri, K. E.,
825   Mazzoleni, L. R., Wozniak, A. S., Bluhm, H., Mysak, E. R., Smith, J. D., Kolb, C. E., and Worsnop, D.
826   R.: Carbon oxidation state as a metric for describing the chemistry of atmospheric organic
827   aerosol, Nat. Chem., 3(2), 133–139, doi:10.1038/nchem.948, 2011.
828 Kukkonen, J., Pohjola, M., Ssokhi, R., Luhana, L., Kitwiroon, N., Fragkou, L., Rantamaki, M., Berge, E.,
829   Odegaard, V., and Havardslordal, L.: Analysis and evaluation of selected local-scale PM air
830   pollution episodes in four European cities: Helsinki, London, Milan and Oslo, Atmos. Environ.,
831   39(15), 2759–2773, doi:10.1016/j.atmosenv.2004.09.090, 2005.
832 Kundu, S., Kawamura, K., Andreae, T. W., Hoffer, A., and Andreae, M. O.: Molecular distributions of
833   dicarboxylic acids, ketocarboxylic acids and α-dicarbonyls in biomass burning aerosols:
834   implications for photochemical production and degradation in smoke layers, Atmos. Chem.
835   Phys., 10(5), 2209–2225, doi:10.5194/acp-10-2209-2010, 2010.
836 Lanz, V. A., Alfarra, M. R., Baltensperger, U., Buchmann, B., Hueglin, C., and Prévôt, A. S. H.: Source
837   apportionment of submicron organic aerosols at an urban site by factor analytical modelling of
838   aerosol mass spectra, Atmos. Chem. Phys., 7(6), 1503–1522, doi:10.5194/acp-7-1503-2007,
839   2007.
840 Lanz, V. A., Prévôt, A. S. H., Alfarra, M. R., Weimer, S., Mohr, C., DeCarlo, P. F., Gianini, M. F. D., Hueglin,
841   C., Schneider, J., Favez, O., D'Anna, B., George, C., and Baltensperger, U.: Characterization of
842   aerosol chemical composition with aerosol mass spectrometry in Central Europe: an overview,
843   Atmos. Chem. Phys., 10(21), 10453–10471, 2010.
844 Larsen, B. R., Gilardoni, S., Stenström, K., Niedzialek, J., Jimenez, J., and Belis, C. A.: Sources for PM air
845   pollution in the Po Plain, Italy: II. Probabilistic uncertainty characterization and sensitivity

Atmospheric
Chemistry
and Physics
Discussions

Open Access

846   analysis of secondary and primary sources, Atmos. Environ., 50, 203–213,
847   doi:10.1016/j.atmosenv.2011.12.038, 2012.
848 Larssen, S., Sluyter, R., and Helmis, C.: Criteria for EUROAIRNET, the EEA Air Quality Monitoring and
849   Information Network, available at:
850   http://www.eea.europa.eu/publications/TEC12/at_download/file (last access: 10 February
851   2016), 1999.
852 Lee, T., Sullivan, A. P., Mack, L., Jimenez, J. L., Kreidenweis, S. M., Onasch, T. B., Worsnop, D. R., Malm,
853   W., Wold, C. E., Hao, W. M., and Collett, J. L.: Chemical smoke marker emissions during flaming
854   and smoldering phases of laboratory open burning of wildland fuels, Aerosol Sci. Tech., 44(9), i–
855   v, doi:10.1080/02786826.2010.499884, 2010.
856 Liu, P. S. K., Deng, R., Smith, K. A., Williams, L. R., Jayne, J. T., Canagaratna, M. R., Moore, K., Onasch, T.
857   B., Worsnop, D. R., and Deshler, T.: Transmission efficiency of an aerodynamic focusing lens
858   system: comparison of model calculations and laboratory measurements for the Aerodyne
859   aerosol mass spectrometer, Aerosol Sci. Tech., 41(8), 721–733,
860   doi:10.1080/02786820701422278, 2007.
861 Maimone, F., Turpin, B. J., Solomon, P., Meng, Q., Robinson, A. L., Subramanian, R., and Polidori, A.:
862   Correction methods for organic carbon artifacts when using quartz-fiber filters in large
863   particulate matter monitoring networks: the regression method and other options, J. Air Waste
864   Manage. Assoc., 61(6), 696–710, doi:10.3155/1047-3289.61.6.696, 2011.
865 McMurry, P. H., Wang, X., Park, K., and Ehara, K.: The relationship between mass and mobility for
866   atmospheric particles: a new technique for measuring particle density, Aerosol Sci. Tech., 36(2),
867   227–238, doi:10.1080/027868202753504083, 2002.
868 Middlebrook, A. M., Bahreini, R., Jimenez, J. L., and Canagaratna, M. R.: Evaluation of composition-
869   dependent collection efficiencies for the Aerodyne aerosol mass spectrometer using field data,
870   Aerosol Sci. Tech., 46(3), 258–271, doi:10.1080/02786826.2011.620041, 2012.
871 Miljevic, B., Heringa, M. F., Keller, A., Meyer, N. K., Good, J., Lauber, A., Decarlo, P. F., Fairfull-Smith, K.
872   E., Nussbaumer, T., Burtscher, H., Prévôt, A. S. H., Baltensperger, U., Bottle, S. E., and Ristovski,
873   Z. D.: Oxidative potential of logwood and pellet burning particles assessed by a novel
874   profluorescent nitroxide probe, Environ. Sci. Technol., 44(17), 6601–6607, 2010.
875 Minguillón, M. C., Ripoll, A., Pérez, N., Prévôt, A. S. H., Canonaco, F., Querol, X., and Alastuey, A.:
876   Chemical characterization of submicron regional background aerosols in the western
877   Mediterranean using an aerosol chemical speciation monitor, Atmos. Chem. Phys., 15(11),
878   6379–6391, doi:10.5194/acp-15-6379-2015, 2015.
879 Naeher, L. P., Brauer, M., Lipsett, M., Zelikoff, J. T., Simpson, C. D., Koenig, J. Q., and Smith, K. R.:
880   Woodsmoke health effects: a review, Inhal. Toxicol., 19(1), 67–106,
881   doi:10.1080/08958370600985875, 2007.
882 Ng, N. L., Herndon, S. C., Trimborn, A., Canagaratna, M. R., Croteau, P. L., Onasch, T. B., Sueper, D.,
883   Worsnop, D. R., Zhang, Q., Sun, Y. L., and Jayne, J. T.: An aerosol chemical speciation monitor
884   (ACSM) for routine monitoring of the composition and mass concentrations of ambient aerosol,
885   Aerosol Sci. Tech., 45(7), 780–794, doi:10.1080/02786826.2011.560211, 2011a.
886 Ng, N. L., Canagaratna, M. R., Jimenez, J. L., Chhabra, P. S., Seinfeld, J. H., and Worsnop, D. R.: Changes in
887   organic aerosol composition with aging inferred from aerosol mass spectra, Atmos. Chem. Phys.,
888   11(13), 6465–6474, doi:10.5194/acp-11-6465-2011, 2011b.
889 Ng, N. L., Canagaratna, M. R., Jimenez, J. L., Zhang, Q., Ulbrich, I. M., and Worsnop, D. R.: Real-time
890   methods for estimating organic component mass concentrations from aerosol mass
891   spectrometer data, Environ. Sci. Technol., 45(3), 910–916, doi:10.1021/es102951k, 2011c.
892 Paatero, P.: User's guide for the multilinear engine program "ME2" for fitting multilinear and
893   quasimultilinear models, University of Helsinki, Finland, 2000.

894 Paatero, P. and Tapper, U.: Positive matrix factorization - a nonnegative factor model with optimal
895   utilization of error-estimates of data values, Environmetrics, 5(2), 111–126,
896   doi:10.1002/env.3170050203, 1994.
897 Paglione, M., Saarikoski, S., Carbone, S., Hillamo, R., Facchini, M. C., Finessi, E., Giulianelli, L., Carbone,
898   C., Fuzzi, S., Moretti, F., Tagliavini, E., Swietlicki, E., Eriksson Stenström, K., Prévôt, A. S. H.,
899   Massoli, P., Canaragatna, M., Worsnop, D., and Decesari, S.: Primary and secondary biomass
900   burning aerosols determined by proton nuclear magnetic resonance (^{1}H-NMR) spectroscopy
901   during the 2008 EUCAARI campaign in the Po Valley (Italy), Atmos. Chem. Phys., 14(10), 5089–
902   5110, doi:10.5194/acp-14-5089-2014, 2014.
903 Pernigotti, D., Georgieva, E., Thunis, P., and Bessagnet, B.: Impact of meteorology on air quality
904   modeling over the Po valley in northern Italy, Atmos. Environ., 51, 303–310,
905   doi:10.1016/j.atmosenv.2011.12.059, 2012.
906 Perrone, M. G., Larsen, B. R., Ferrero, L., Sangiorgi, G., De Gennaro, G., Udisti, R., Zangrando, R.,
907   Gambaro, A., and Bolzacchini, E.: Sources of high $PM_{2.5}$ concentrations in Milan, northern Italy:
908   molecular marker data and CMB modelling, Sci. Total Environ., 414, 343–355,
909   doi:10.1016/j.scitotenv.2011.11.026, 2012.
910 Petit, J.-E., Favez, O., Sciare, J., Crenn, V., Sarda-Estève, R., Bonnaire, N., Močnik, G., Dupont, J.-C.,
911   Haeffelin, M., and Leoz-Garziandia, E.: Two years of near real-time chemical composition of
912   submicron aerosols in the region of Paris using an aerosol chemical speciation monitor (ACSM)
913   and a multi-wavelength aethalometer, Atmos. Chem. Phys., 15, 2985–3005, doi:10.5194/acp-15-
914   2985-2015, 2015.
915 Pitz, M., Cyrys, J., Karg, E., Wiedensohler, A., Wichmann, H.-E., and Heinrich, J.: Variability of apparent
916   particle density of an urban aerosol, Environ. Sci. Technol., 37(19), 4336–4342,
917   doi:10.1021/es034322p, 2003.
918 Pitz, M., Schmid, O., Heinrich, J., Birmili, W., Maguhn, J., Zimmermann, R., Wichmann, H.-E., Peters, A.,
919   and Cyrys, J.: Seasonal and diurnal variation of $PM_{2.5}$ apparent particle density in urban air in
920   Augsburg, Germany, Environ. Sci. Technol., 42(14), 5087–5093, 2008.
921 Putaud, J. P., Van Dingenen, R., and Raes, F.: Submicron aerosol mass balance at urban and semirural
922   sites in the Milan area (Italy), J. Geophys. Res.-Atmos., 107(D22), LOP 11–1–LOP 11–10,
923   doi:10.1029/2000JD000111, 2002.
924 Putaud, J.-P., Van Dingenen, R., Alastuey, A., Bauer, H., Birmili, W., Cyrys, J., Flentje, H., Fuzzi, S., Gehrig,
925   R., Hansson, H. C., Harrison, R. M., Herrmann, H., Hitzenberger, R., Huglin, C., Jones, A. M.,
926   Kasper-Giebl, A., Kiss, G., Kousa, A., Kuhlbusch, T. A. J., Loschau, G., Maenhaut, W., Molnar, A.,
927   Moreno, T., Pekkanen, J., Perrino, C., Pitz, M., Puxbaum, H., Querol, X., Rodriguez, S., Salma, I.,
928   Schwarz, J., Smolik, J., Schneider, J., Spindler, G., ten Brink, H., Tursic, J., Viana, M.,
929   Wiedensohler, A., and Raes, F.: A European aerosol phenomenology – 3: physical and chemical
930   characteristics of particulate matter from 60 rural, urban, and kerbside sites across Europe,
931   Atmos. Environ., 44, 1308–1320, 2010.
932 Putaud, J.-P., Adam, M., Belis, C. A., Bergamaschi, P., Cancellinha, J., Cavalli, F., Cescatti, A., Daou, D.,
933   Dell'Acqua, A., Douglas, K., Duerr, M., Goded, I., Grassi, F., Gruening, C., Hjorth, J., Jensen, N. R.,
934   Lagler, F., Manca, G., Martins Dos Santos, S., Passarella, R., Pedroni, V., Rocha e Abreu, P., Roux,
935   D., Scheeren, B., and Schembari, C.: JRC-Ispra Atmosphere-Biosphere-Climate Integrated
936   monitoring Station (ABC-IS): 2011 report, JRC Technical Reports, Joint Research Centre, Ispra
937   (Italy), available at:
938   http://publications.jrc.ec.europa.eu/repository/bitstream/111111111/28242/1/lb-na-25753-en-
939   n.pdf (last access: 28 March 2014), 2013.
940 Putaud, J.-P., Bergamaschi, P., Bressi, M., Cavalli, F., Cescatti, A., Daou, D., Dell'acqua, A., Douglas, K.,
941   Duerr, M., Fumagalli, I., Goded Ballarin, I., Grassi, F., Gruening, C., Hjorth, J., Jensen, N., Lagler,

942   F., Manca, G., Martins Dos Santos, S., Matteucci, M., Passarella, R., Pedroni, V., Pokorska, O.,
943   and Roux, D.: JRC – Ispra Atmosphere – Biosphere – Climate Integrated monitoring Station 2013
944   report, EUR - Scientific and Technical Research Reports, Publications Office of the European
945   Union, available at: http://publications.jrc.ec.europa.eu/repository/handle/111111111/33904
946   (last access: 19 February 2015), 2014a.
947 Putaud, J. P., Cavalli, F., Martins dos Santos, S., and Dell'Acqua, A.: Long-term trends in aerosol optical
948   characteristics in the Po Valley, Italy, Atmos. Chem. Phys., 14(17), 9129–9136, doi:10.5194/acp-
949   14-9129-2014, 2014b.
950 Reiss, R., Anderson, E. L., Cross, C. E., Hidy, G., Hoel, D., McClellan, R., and Moolgavkar, S.: Evidence of
951   health impacts of sulfate- and nitrate-containing particles in ambient air, Inhal. Toxicol., 19(5),
952   419–449, doi:10.1080/08958370601174941, 2007.
953 Riffault, V., Zhang, S., Tison, E., and Setyan, A.: Chloride RIE measurements, 14th AMS user meeting, 8
954   September 2013, available at: http://cires.colorado.edu/jimenez-
955   group/UsrMtgs/UsersMtg14/AMS_user_meeting_Chl_RIE_riffault.pdf (last access: 10 February
956   2016), 2013.
957 Ripoll, A., Minguillón, M. C., Pey, J., Jimenez, J. L., Day, D. A., Sosedova, Y., Canonaco, F., Prévôt, A. S. H.,
958   Querol, X., and Alastuey, A.: Long-term real-time chemical characterization of submicron
959   aerosols at Montsec (southern Pyrenees, 1570 m a.s.l.), Atmos. Chem. Phys., 15(6), 2935–2951,
960   doi:10.5194/acp-15-2935-2015, 2015.
961 Saarikoski, S., Carbone, S., Decesari, S., Giulianelli, L., Angelini, F., Canagaratna, M., Ng, N. L., Trimborn,
962   A., Facchini, M. C., Fuzzi, S., Hillamo, R., and Worsnop, D.: Chemical characterization of
963   springtime submicrometer aerosol in Po Valley, Italy, Atmos. Chem. Phys., 12(18), 8401–8421,
964   doi:10.5194/acp-12-8401-2012, 2012.
965 Schaap, M., Van Loon, M., Ten Brink, H. M., Dentener, F. J., and Builtjes, P. J. H.: Secondary inorganic
966   aerosol simulations for Europe with special attention to nitrate, Atmos. Chem. Phys., 4(3), 857–
967   874, 2004.
968 Schlesinger, R. B. and Cassee, F.: Atmospheric secondary inorganic particulate matter: the toxicological
969   perspective as a basis for health effects risk assessment, Inhal. Toxicol., 15(3), 197–235,
970   doi:10.1080/08958370390168247, 2003.
971 Seinfeld, J. H. and Pandis, S. N.: Atmospheric Chemistry and Physics: from Air Pollution to Climate
972   Change, Wiley, New York, USA, 2006.
973 Sturtz, T. M., Adar, S. D., Gould, T., and Larson, T. V.: Constrained source apportionment of coarse
974   particulate matter and selected trace elements in three cities from the multi-ethnic study of
975   atherosclerosis, Atmos. Environ., 84, 65–77, doi:10.1016/j.atmosenv.2013.11.031, 2014.
976 Sun, Y., Wang, Z., Dong, H., Yang, T., Li, J., Pan, X., Chen, P., and Jayne, J. T.: Characterization of summer
977   organic and inorganic aerosols in Beijing, China with an aerosol chemical speciation monitor,
978   Atmos. Environ., 51, 250–259, doi:10.1016/j.atmosenv.2012.01.013, 2012.
979 Takegawa, N., Miyazaki, Y., Kondo, Y., Komazaki, Y., Miyakawa, T., Jimenez, J. L., Jayne, J. T., Worsnop, D.
980   R., Allan, J. D., and Weber, R. J.: Characterization of an Aerodyne aerosol mass spectrometer
981   (AMS): intercomparison with other aerosol instruments, Aerosol Sci. Tech., 39(8), 760–770,
982   doi:10.1080/02786820500243404, 2005.
983 Takegawa, N., Miyakawa, T., Kondo, Y., Jimenez, J. L., Zhang, Q., Worsnop, D. R., and Fukuda, M.:
984   Seasonal and diurnal variations of submicron organic aerosol in Tokyo observed using the
985   Aerodyne aerosol mass spectrometer, J. Geophys. Res.-Atmos., 111(D11), D11206,
986   doi:10.1029/2005JD006515, 2006.
987 Turpin, B. J. and Lim, H. J.: Species contributions to $PM_{2.5}$ mass concentrations: revisiting common
988   assumptions for estimating organic mass, Aerosol Sci. Tech., 35(1), 602–610,
989   doi:10.1080/02786820152051454, 2001.

Atmospheric
Chemistry
and Physics
Discussions

Open Access

EGU

990   Turpin, B. J., Saxena, P., and Andrews, E.: Measuring and simulating particulate organics in the
991   atmosphere: problems and prospects, Atmos. Environ., 34(18), 2983–3013, 2000.
992   Ulbrich, I. M., Canagaratna, M. R., Zhang, Q., Worsnop, D. R., and Jimenez, J. L.: Interpretation of organic
993   components from positive matrix factorization of aerosol mass spectrometric data, Atmos.
994   Chem. Phys., 9(9), 2891–2918, 2009.
995   Ulbrich, I. M., Lechner, M., and Jimenez, J. L.: AMS Spectral Database, available at:
996   http://cires.colorado.edu/jimenez-group/AMSsd/ (last access: 7 October 2015), 2015.
997   van Donkelaar, A., Martin, R. V., Brauer, M., Kahn, R., Levy, R., Verduzco, C., and Villeneuve, P. J.: Global
998   estimates of ambient fine particulate matter concentrations from satellite-based aerosol optical
999   depth: development and application, Environ. Health Persp., 118(6), 847–855,
1000   doi:10.1289/ehp.0901623, 2010.
1001   Volkamer, R., Jimenez, J. L., San Martini, F., Dzepina, K., Zhang, Q., Salcedo, D., Molina, L. T., Worsnop, D.
1002   R., and Molina, M. J.: Secondary organic aerosol formation from anthropogenic air pollution:
1003   rapid and higher than expected, Geophys. Res. Lett., 33(17), doi:10.1029/2006GL026899, 2006.
1004   Watson, J. G., Chow, J. C., Chen, L.-W. A., and Frank, N. H.: Methods to assess carbonaceous aerosol
1005   sampling artifacts for IMPROVE and other long-term networks, J. Air Waste Manage. Assoc.,
1006   59(8), 898–911, doi:10.3155/1047-3289.59.8.898, 2009.
1007   Weimer, S., Drewnick, F., Hogrefe, O., Schwab, J. J., Rhoads, K., Orsini, D., Canagaratna, M., Worsnop, D.
1008   R., and Demerjian, K. L.: Size-selective nonrefractory ambient aerosol measurements during the
1009   particulate matter technology assessment and characterization study - New York 2004 winter
1010   intensive in New York City, J. Geophys. Res., 111(D18), doi:10.1029/2006JD007215, 2006.
1011   WHO: WHO Air quality guidelines for particulate matter, ozone, nitrogen dioxide and sulfur dioxide:
1012   global update 2005: summary of risk assessment, available at:
1013   http://apps.who.int/iris/handle/10665/69477 (last access: 10 October 2014), 2006.
1014   WHO: Review of evidence on health aspects of air pollution_ REVIHAAP Project, Technical Report,
1015   available at: http://www.euro.who.int/__data/assets/pdf_file/0004/193108/REVIHAAP-Final-
1016   technical-report-final-version.pdf (last access: 15 April 2015), 2013.
1017   Wiedensohler, A., Birmili, W., Nowak, A., Sonntag, A., Weinhold, K., Merkel, M., Wehner, B., Tuch, T.,
1018   Pfeifer, S., Fiebig, M., Fjäraa, A. M., Asmi, E., Sellegri, K., Depuy, R., Venzac, H., Villani, P., Laj, P.,
1019   Aalto, P., Ogren, J. A., Swietlicki, E., Williams, P., Roldin, P., Quincey, P., Hüglin, C., Fierz-
1020   Schmidhauser, R., Gysel, M., Weingartner, E., Riccobono, F., Santos, S., Grüning, C., Faloon, K.,
1021   Beddows, D., Harrison, R., Monahan, C., Jennings, S. G., O'Dowd, C. D., Marinoni, A., Horn, H.-G.,
1022   Keck, L., Jiang, J., Scheckman, J., McMurry, P. H., Deng, Z., Zhao, C. S., Moerman, M., Henzing, B.,
1023   de Leeuw, G., Löschau, G., and Bastian, S.: Mobility particle size spectrometers: harmonization
1024   of technical standards and data structure to facilitate high quality long-term observations of
1025   atmospheric particle number size distributions, Atmos. Meas. Tech., 5(3), 657–685,
1026   doi:10.5194/amt-5-657-2012, 2012.
1027   WMO, Zhu, T., Melamed, M., Parrish, D., Gauss, M., Gallardo Klenner, L., Lawrence, M., Konare, A., and
1028   Liousse, C.: WMO/IGAC impacts of megacities on air pollution and climate, available at:
1029   http://www.igacproject.org/sites/all/themes/bluemasters/images/GAW Report 205.pdf (last
1030   access: 29 July 2015), 2012.
1031   Zhang, Q.: Time- and size-resolved chemical composition of submicron particles in Pittsburgh:
1032   implications for aerosol sources and processes, J. Geophys. Res., 110(D7),
1033   doi:10.1029/2004JD004649, 2005.
1034   Zhang, Q., Jimenez, J. L., Canagaratna, M. R., Allan, J. D., Coe, H., Ulbrich, I., Alfarra, M. R., Takami, A.,
1035   Middlebrook, A. M., Sun, Y. L., Dzepina, K., Dunlea, E., Docherty, K., DeCarlo, P. F., Salcedo, D.,
1036   Onasch, T., Jayne, J. T., Miyoshi, T., Shimono, A., Hatakeyama, S., Takegawa, N., Kondo, Y.,
1037   Schneider, J., Drewnick, F., Borrmann, S., Weimer, S., Demerjian, K., Williams, P., Bower, K.,

Atmospheric
Chemistry
and Physics
Open Access
Discussions

EGU

1038   Bahreini, R., Cottrell, L., Griffin, R. J., Rautiainen, J., Sun, J. Y., Zhang, Y. M., and Worsnop, D. R.:
1039   Ubiquity and dominance of oxygenated species in organic aerosols in anthropogenically-
1040   influenced Northern Hemisphere midlatitudes, Geophys. Res. Lett., 34(13),
1041   doi:10.1029/2007GL029979, 2007.
1042 Zhang, Q., Jimenez, J. L., Canagaratna, M. R., Ulbrich, I. M., Ng, N. L., Worsnop, D. R., and Sun, Y.:
1043   Understanding atmospheric organic aerosols via factor analysis of aerosol mass spectrometry: a
1044   review, Anal. Bioanal. Chem., 401(10), 3045–3067, doi:10.1007/s00216-011-5355-y, 2011.

Atmospheric
Chemistry
and Physics
Discussions

Open Access

EGU

1045 **Tables and Figures**

1046

1047 Table 1. Consistency of ACSM measurements: comparison between ACSM and independent analytical techniques using orthogonal regression

1048 analyses. Slopes and intercepts are indicated ± uncertainties.

1049

|	r^2					slope					intercept				
	Sp	Su	Au	Wi	An	Sp	Su	Au	Wi	An	Sp	Su	Au	Wi	An
Org vs OC	0.91	0.90	0.86	0.92	0.77	2.18 ± 0.07	2.92 ± 0.10	1.87 ± 0.09	1.26 ± 0.04	1.72 ± 0.04	-0.29 ± 0.37	-1.07 ± 0.32	-0.28 ± 0.36	0.74 ± 0.37	0.61 ± 0.25
Nitrate	0.95	0.53	0.96	0.92	0.91	1.37 ± 0.03	4.27 ± 0.25	1.28 ± 0.03	0.86 ± 0.03	1.28 ± 0.02	0.42 ± 0.18	0.64 ± 0.11	0.48 ± 0.10	0.62 ± 0.11	0.48 ± 0.09
Sulfate	0.96	0.97	0.92	0.86	0.95	1.05 ± 0.02	0.98 ± 0.02	0.96 ± 0.04	1.38 ± 0.06	1.00 ± 0.01	-0.01 ± 0.04	0.02 ± 0.06	0.04 ± 0.07	-0.25 ± 0.06	0.00 ± 0.03
Ammonium	0.92	0.70	0.91	0.95	0.90	1.03 ± 0.03	1.00 ± 0.06	0.93 ± 0.04	0.81 ± 0.02	0.99 ± 0.02	-0.04 ± 0.07	-0.04 ± 0.07	-0.12 ± 0.05	0.03 ± 0.03	-0.08 ± 0.03
Chloride	0.75	0.00	0.59	0.78	0.52	2.68 ± 0.13	-0.13 ± 0.09	0.68 ± 0.06	1.13 ± 0.07	1.75 ± 0.06	0.04 ± 0.01	0.03 ± 0.00	0.04 ± 0.00	-0.02 ± 0.01	0.02 ± 0.01
Mass vs volume	0.87	0.82	0.88	0.85	0.81	1.91 ± 0.01	1.95 ± 0.02	1.45 ± 0.01	1.34 ± 0.01	1.63 ± 0.01	-1.16 ± 0.19	-1.36 ± 0.18	-2.45 ± 0.19	-0.11 ± 0.20	-1.09 ± 0.11

1050

1051

1052 Legend: Sp: spring (March-April-May), Su: summer (June-July-August), Au: autumn (September-October-November), Wi: winter (December-

1053 January-February), An: annual. Independent analytical techniques refer to i) EC-OC Sunset Analyzer for OC from $PM_{2.5}$ sampling, ii) Ion

1054 Chromatography for ions from $PM_{2.5}$ sampling and iii) DMPS for volume concentrations (see Sect. 2.3 for more details). Mass refers to NR-

1055 PM_1+BC. Intercepts are in $\mu g/m^3$. Slopes of mass vs volume are in g/cm^3 and dimensionless otherwise.

Atmospheric
Chemistry
and Physics
Open Access
Discussions
EGU

1056   Table 2. Comparison (coefficient of determination, r^2) between SA factors, organic m/z tracers and independent species time series. BC stands

1057   for Black Carbon; Org_i stands for organic signal at m/z i (i=43, 44, 60, 67, 73, 81).

1058

	HOA					BBOA					OOA				
	Org_67	Org_81	NOx	CO	BC	Org_60	Org_73	NOx	CO	BC	Org_43	Org_44	NH4	SO4	NO3
SPRING	0.60	0.55	0.03	0.08	0.28	0.99	0.97	0.32	0.81	0.70	0.88	0.94	0.76	0.43	0.77
SUMMER	0.90	0.91	0.07	0.40	0.52			-			0.97	0.94	0.54	0.60	0.19
AUTUMN	0.63	0.61	0.07	0.10	0.24	0.99	0.97	0.06	0.68	0.47	0.82	0.92	0.47	0.53	0.38
WINTER	0.58	0.57	0.34	0.33	0.39	0.98	0.97	0.20	0.66	0.63	0.80	0.99	0.50	0.39	0.66

1059
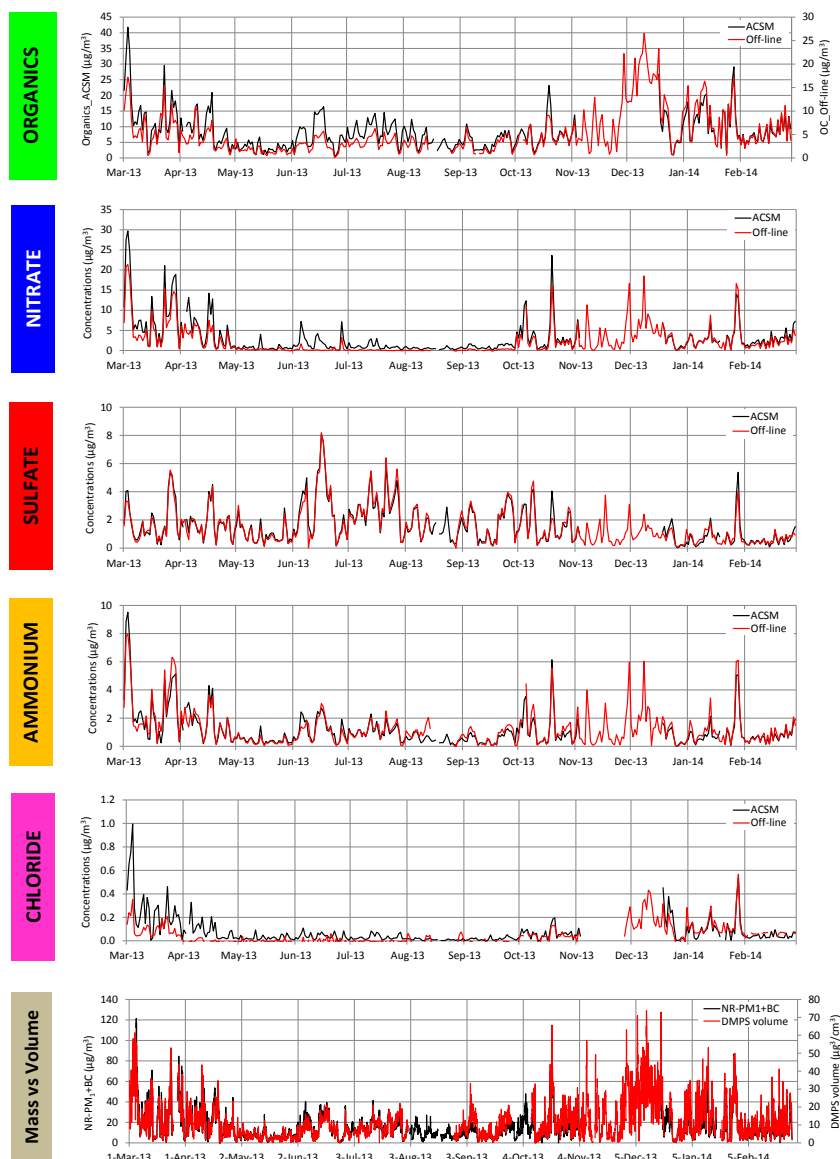
1060

Figure 1. Comparison between measurements performed with the ACSM and other co-located analytical

techniques. See Table 1 and Sect. 2.3 for more details.
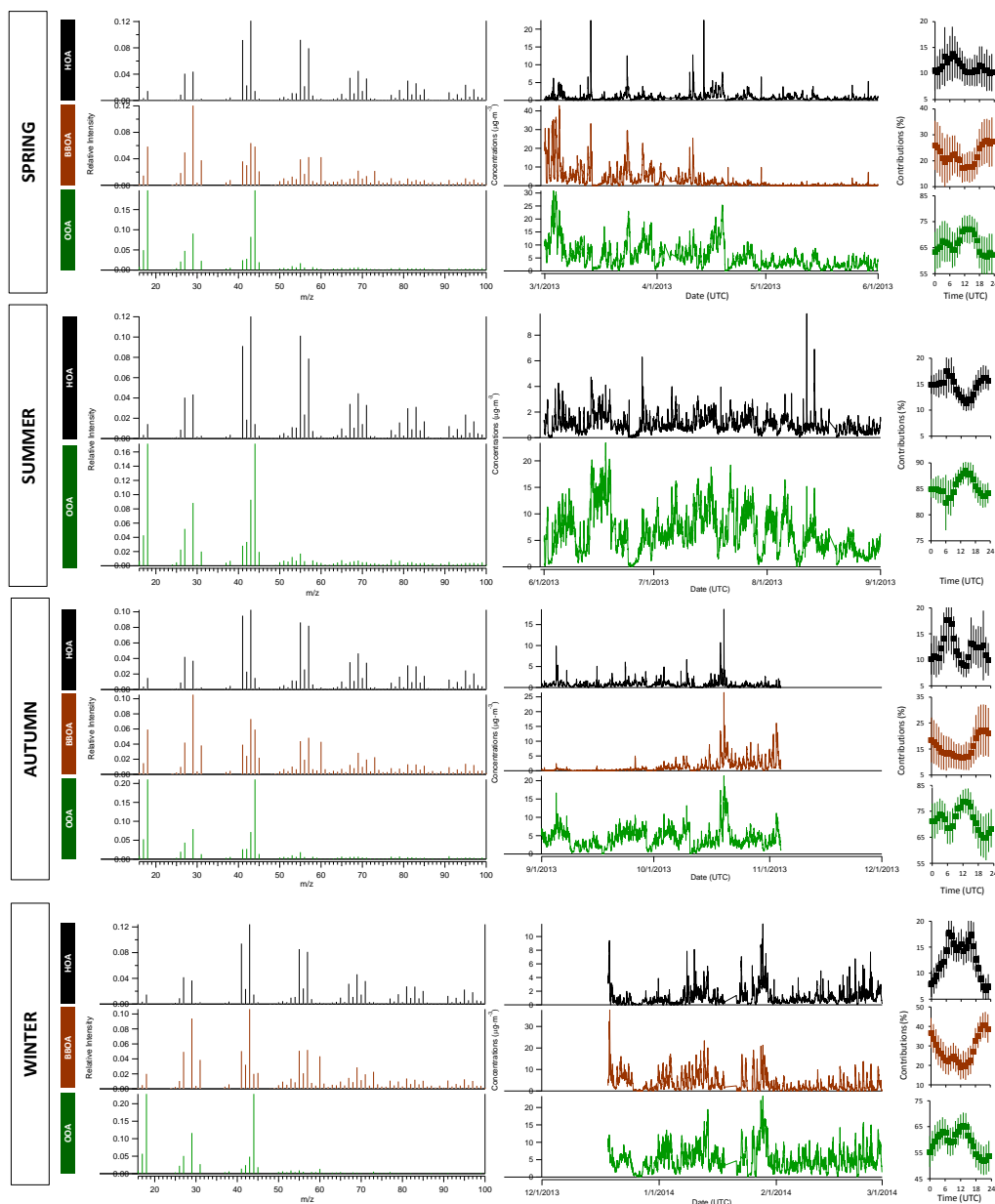
1063


Figure 2. Organic source apportionment presented by season: factor profiles (left), time series (middle) and daily cycles (right, error bars represent 1 standard deviation). Seasons are defined as Spring: MAM, Summer: JJA, Autumn: SON and Winter: DJF.
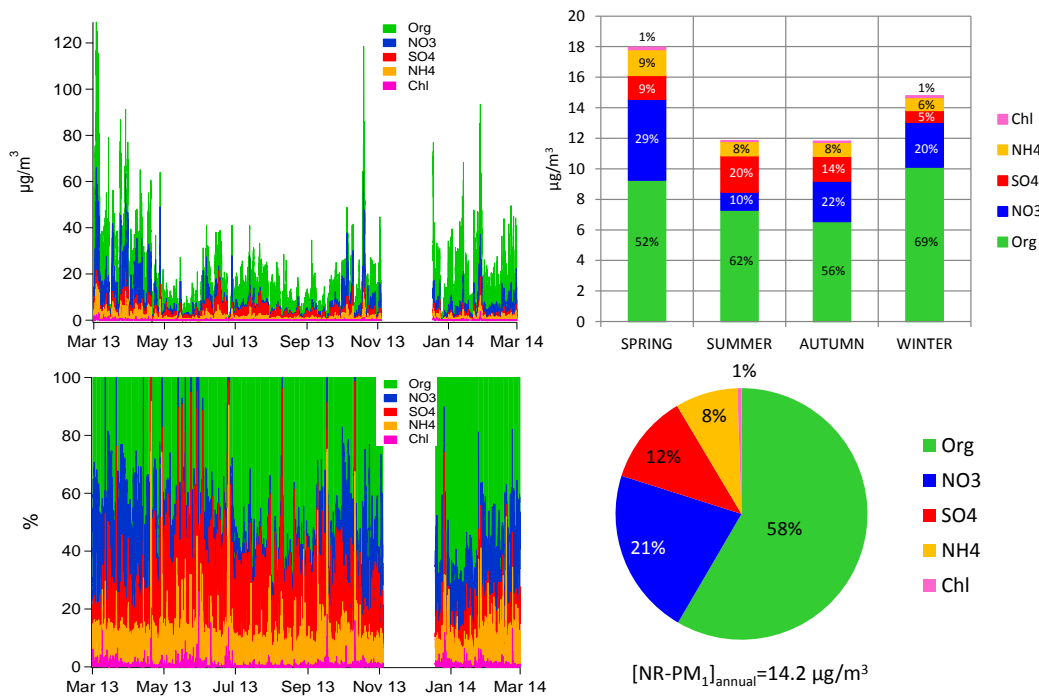
1067

Figure 3. Overview of the chemical composition of NR-PM$_1$ at Ispra (Po Valley, Italy). Left: absolute (top)
and relative (bottom) chemical composition with 30 min time resolution; top right: absolute seasonal
average, bottom right: annual average.

Atmospheric
Chemistry
and Physics
Discussions
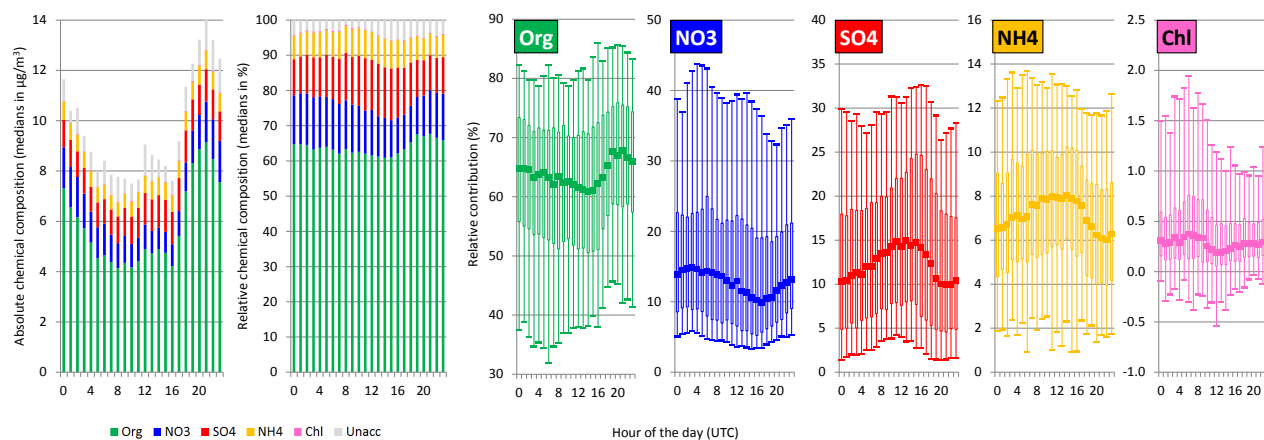
1071

1072   Figure 4. Daily cycles of NR-PM$_1$ chemical composition on the annual scale. Unacc: unaccounted mass, whisker plots are constructed from the

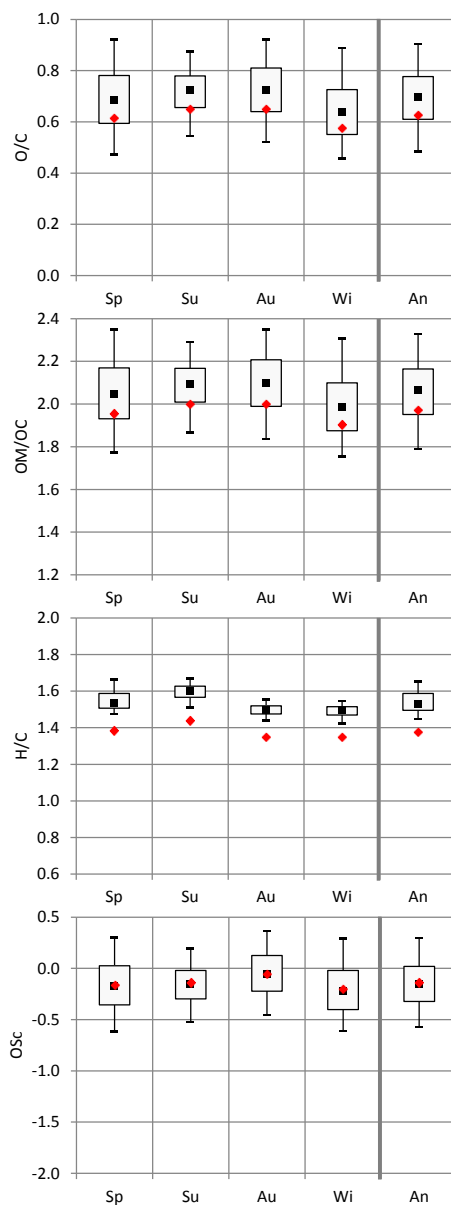1073   5th, 25th, 50th, 75th and 95th percentiles.
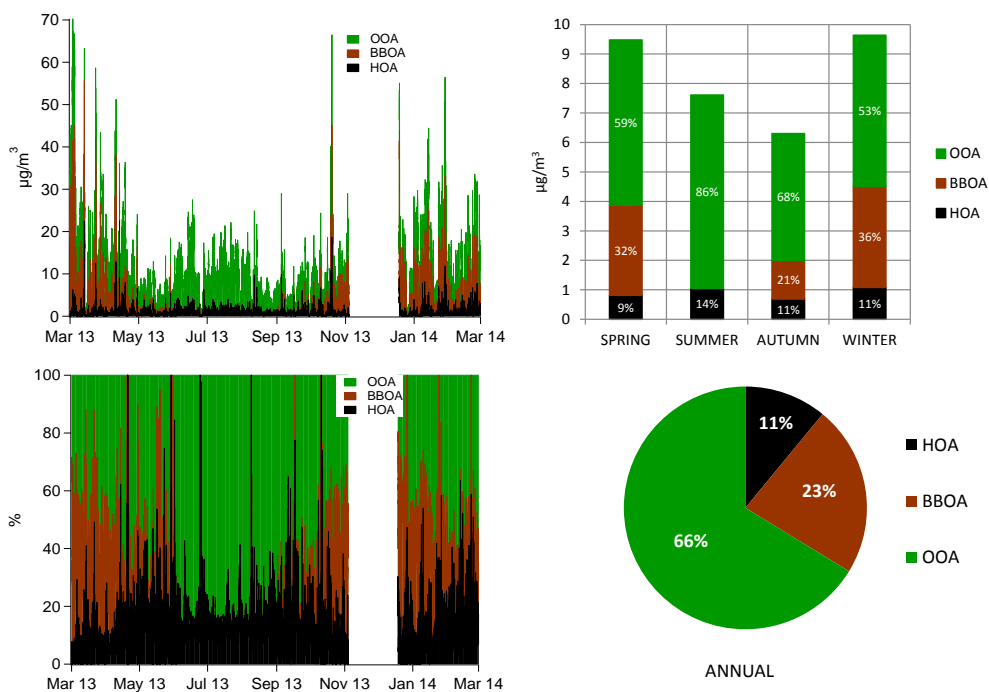
1074

Figure 5. Overview of HOA, BBOA and OOA contributions to organic aerosols; see legend Figure 3.

Atmospheric
Chemistry
and Physics
Discussions
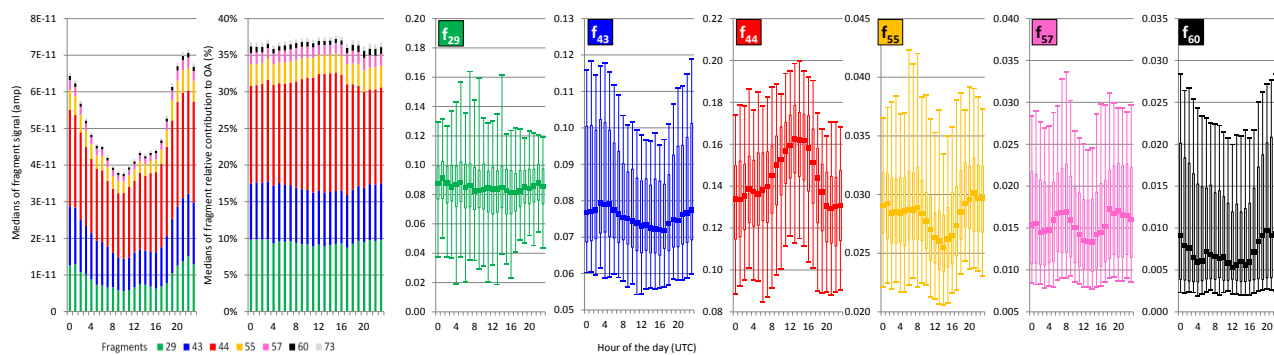
1076

1077   Figure 6. Annual statistics describing the daily cycles of the major organic fragments. Box plots are constructed from the 5th, 25th, 50th, 75th and

1078   95th percentiles.

Atmospheric
Chemistry
and Physics
Discussions

Open Access

EGU

Figure 7. Seasonal and annual O/C, OM/OC, H/C and OSc of ambient OA. Sp: spring (MAM), Su: summer
(JJA), Au: autumn (SON), Wi: winter (DJF), An: annual. Black: 5th, 25th, 50th, 75th and 95th percentiles
estimates following Canagaratna et al. (2015); red: median estimates following Aiken et al. (2008) for
O/C and OM/C, Ng et al. (2011b) for H/C and Aiken et al. (2008), Kroll et al. (2011) and Ng et al. (2011b)
for OSc. Note that the authors do not recommend comparing absolute O/C, OM/OC and OSc values
reported here with other AMS studies, given the uncertainties associated with f_{44} quantifications from
ACSM measurements (please see text).
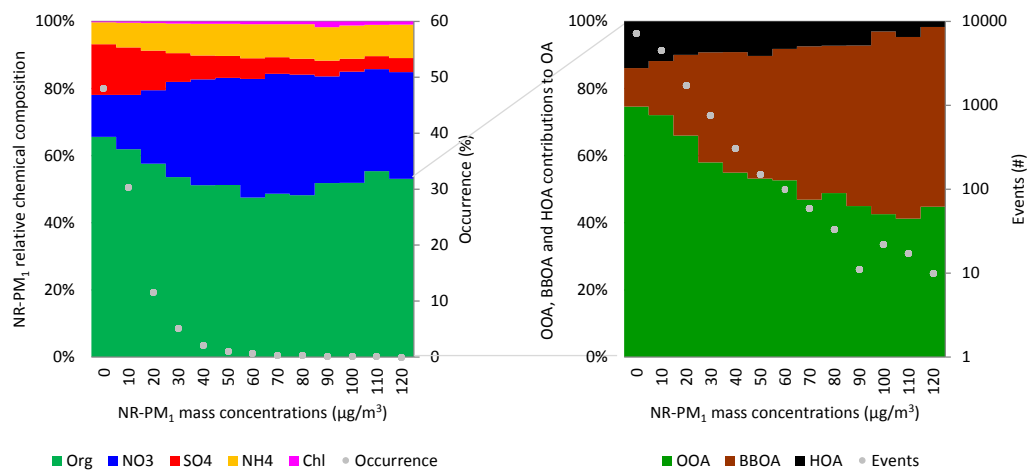
1087

Figure 8. NR-PM$_1$ relative chemical composition (left) and OA factor contributions (right) averages in function of NR-PM$_1$ mass concentrations (bins of 10 µg/m^3). Occurrence (%, left) and number of events (#, right) are indicated (solid dots) for each NR-PM$_1$ bin. Note that one event corresponds to one 30 minute average.